2016

Poly(arylene Ether Sulfone)s with Ammonium Groups Located on Pendent Phenyl Sulfonyl Moieties for Anionic Exchange Membranes

Trevor I. Schumacher
Wright State University

Poly(arylene ether sulfone)s with Ammonium Groups Located on Pendent Phenyl Sulfonyl Moieties for Anionic Exchange Membranes

A thesis submitted in partial fulfillment of the
requirements for the degree of
Master of Science

By:

TREVOR I. SCHUMACHER
B.S., The Ohio State University, 2012

2016
Wright State University

WRIGHT STATE UNIVERSITY
GRADUATE SCHOOL

June 28, 2016

I HEREBY RECOMMEND THAT THE THESIS PREPARED UNDER MY SUPERVISION BY Trevor I. Schumacher ENTITLED Poly(arylene ether sulfone)s with Ammonium Groups Located on Pendent Phenyl Sulfonyl Moieties for Anionic Exchange Membranes BE ACCEPTED IN PARTIAL FULFILLMENT OF THE REQUIREMENTS FOR THE DEGREE OF Master of Science.

_____
Eric Fossum, Ph.D.
Thesis Advisor

Committee on
Final Examination:

_____
David Grossie, Ph.D.
Chair, Department of Chemistry

_____
Eric Fossum, Ph.D.

_____
William A. Feld, Ph.D.

_____
Kenneth Turnbull, Ph.D.

_____
Robert E. W. Fyfe Ph.D.
Vice President for Research and
Dean of the Graduate School

ABSTRACT

Schumacher, Trevor I. M.S., Department of Chemistry, Wright State University, 2016.
Poly(arylene ether sulfone)s with Ammonium Groups Located on Pendent Phenyl Sulfonyl Moieties for Anionic Exchange Membranes

A series of poly(aryl ether sulfone)s with varying percentages of ammonium groups, located on truly pendent positions, was prepared and characterized. The initial polymers were prepared by nucleophilic aromatic substitution (NAS) polycondensation reactions of varying ratios of 3,5-difluoro-4'-methyldiphenylsulfone and 4,4'-difluorodiphenylsulfone, with bisphenol-A as the nucleophilic reaction partner. The tolyl groups in the resulting polymers were subjected to radical bromination with *N*-bromosuccinimide, followed by amination with three different amines: trimethylamine, dimethylhexadecylamine, and *N*-methylimidazole. The polymers were characterized by ^{1}H and ^{13}C NMR spectroscopy, thermogravimetric analysis, and differential scanning calorimetry. With the exception of the 100% functionalized polymers, tough films were observed after casting from solutions in dimethylformamide. The films were evaluated for potential use as alkaline exchange membranes (AEM) by determining their water uptake and ion exchange capacity values.

TABLE OF CONTENTS

LIST OF FIGURES

Page

LIST OF SCHEMES

LIST OF TABLES

LIST OF EQUATIONS

Page

ACKNOWLEDGEMENTS

I would like to thank my committee members Dr. William Feld, Dr. Kenneth Turnbull, and Dr. Eric Fossum for the information they have instilled in me. I would also like to thank my advisor, Dr. Eric Fossum, for his guidance and patience over the past two years. Thank you to fellow group members, students, faculty, and staff members of Wright State University. This material is based upon work supported by the National Science Foundation under CHE-1307117.

1. INTRODUCTION

1.1 Future of Energy

The world's population is increasing at a fast pace and with this growth comes the demand for more energy. The U.S. Energy Information Administration predicts that the world energy use will increase 56% between the years 2010-2040.[1] In order to meet this escalating energy consumption, mankind is looking at developing different methods of acquiring energy other than those from traditional fossil fuels. Traditional fossil fuels are a non-renewable energy source and it is estimated that at current rates oil, coal, and gas reserves will be depleted in the next 40, 200, and 70 years, respectively, unless more reserves in nature are found.[2] In addition to the decline in fossil fuel stockpiles, these types of fuels have been shown to have a negative environment impact. Environmental concerns include climate change caused by the production of greenhouse gases, contamination from toxic pollutants, and altering geological sub terrain via drilling, mining, and fracking techniques.[3] With the inevitable change from traditional fossil fuels arising, there is a necessity for designing alternative energy approaches that are efficient, eco-friendly, and meet the necessary consumption levels.

The world's future demand for energy cannot be obtained from a single type of source, but rather a mixture of both renewable and non-renewable technologies. Fuel cells are one process that offer a promising alternative energy resource and are currently being researched by academia, industry, and government around the world. The Office of

Energy Efficiency and Renewable Energy invested 10 million dollars in 2015 for 11 projects to promote advances in fuel cell technologies.[4] In recent years, alkaline anionic exchange membrane fuel cells have gained a considerable amount of interest.

1.2 Fuel Cells

William Grove invented the fuel cell in the year 1839. He used an electrochemical process that involved the use of platinum electrodes, aqueous sulfuric acid, oxygen and hydrogen gases. From this device he observed an electrical current and published his results.[5] The invention of the fuel cell was well received by the science community and ultimately led to the development of different types. Fuel cells can be separated into two categories: low temperature and high temperature. Low temperature fuel cells include alkaline, polymer exchange membrane, direct methanol, and phosphoric acid fuel cells. High temperature fuels include molten carbonate, solid oxide fuel cells, and regenerative fuel cells.[6] All of these fuel cells are electro-chemical devices that produce an electrical current that can be captured and used for energy consumption. Fuel cells, in theory, can provide a limitless output of energy as long as there is continuous supply of fuel source, unlike batteries that store a finite amount of energy and are depleted over time from use.[7] Fuel cells differentiate from traditional fossil fuels in offering higher energy conversion efficiencies and also being eco-friendly. Fossil fuels perform at or below a 33% effective energy efficiency whereas fuel cells achieve a 40-65% effective energy efficiency based on the conversion of fuel to usable energy.[8] These characteristics make fuel cells a

promising alternative energy source which can be applicable to an array of areas including utility, transportation, and both stationary or mobile devices.

Willard Grub developed the first polymer exchange membrane fuel cell while working at General Electric in the year 1955. His fuel cell involved the use of a proton exchange membrane that produced an electrical current from a catalytic reaction.[9] This novel idea paved the way for proton exchange membranes and ultimately led to the introduction of alkaline exchange membrane fuel cells.

1.3 Proton Exchange Membrane Fuel Cells

Proton exchange membrane fuel cells (PEMFCs) produce electrical energy through the electro-chemical process of converting hydrogen fuel and oxygen into water as shown in **Figure 1**.[10]

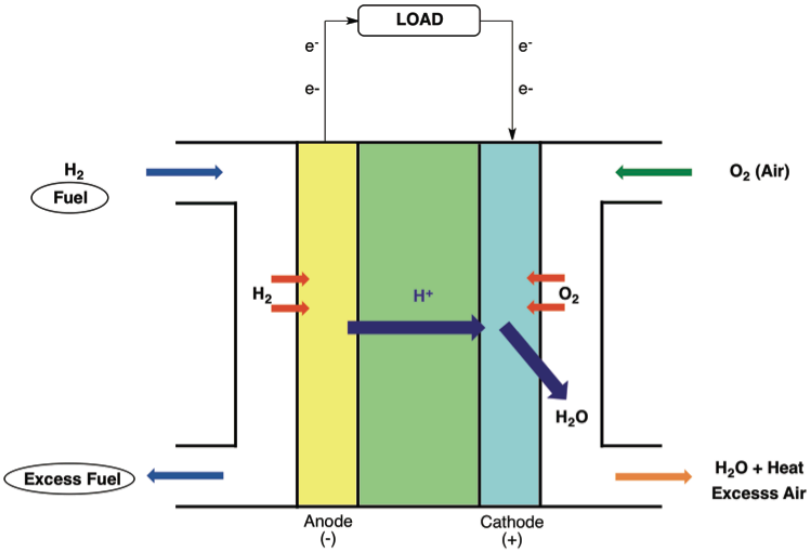

Figure 1. Representation of a PEMFC

The device primarily consists of hydrogen fuel, a catalyst anode, a polymer proton exchange membrane, a catalyst cathode, and oxygen. The hydrogen is initially oxidized at the catalyst anode, causing the hydrogen to be split into electrons and protons. Electrons travel by means of the external circuit towards the cathode and the protons migrate through the anionic polymer membrane via hydrophilic micro-channels by two types of pathways: Grotthus, and vehicular mechanisms.[11,12] The Grotthus mechanism occurs through proton hopping between water molecules (see page 8), whereas in the vehicular mechanism protons diffuse through the system with "vehicles" such as hydronium ions. The protons and electrons ultimately react with oxygen at the cathode to produce water and heat. The half and overall reactions are observed below:

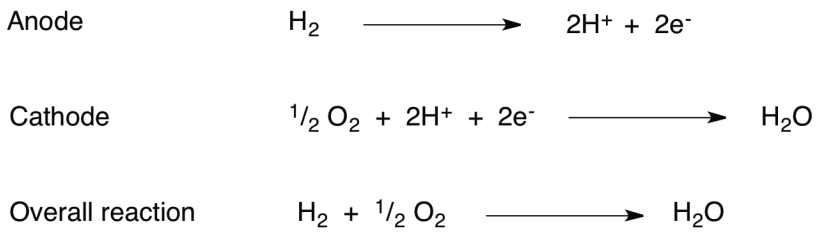

The electrical energy created by the conducting electrons through the external wire can be used to power energy requiring devices. These hydrogen fuel cells provide the necessary energy requirements without creating harmful environmental byproducts as seen by the overall reaction above. Although there have been great advancements in the production of PEMFCs, there are still problems that are associated with their overall

energy output performance and these issues must be fixed before they become commercially viable. The two main difficulties with PEMFCs are associated with the catalyst and the polymer exchange membrane.

1.4 PEMFCs and Disadvantages

The catalyst is typically made of the rare earth metal platinum (0.003 ppm).[50] Platinum is considered to be the most highly efficient electro-chemical catalyst, however it is expensive and toxic gas impurities can be detrimental towards the catalyst-electrode performance while being operated at a low temperature.[13] The U.S. Department of Energy estimated that the amount of platinum used for current PEMFCs must be reduced as much as four fold to even be considered as an alternative to modern, combustion engines.[14] Research must be performed to improve upon platinum catalysts or a cheaper alternative pH-stable, metal catalyst must be designed for practical implementation.

The proton exchange membrane (PEM) consists of a polymer backbone tethered with various types of anionic side groups. The chief principle of the membrane is to only allow for the conduction of protons from the anode to the cathode and to prevent electron, fuel, or oxidant crossover. It is essential for PEMs to maintain good mechanical properties and be operated at elevated temperatures with minimal degradation or water absorption. The U.S. department of Energy has enacted a set of standards for current PEMs to be operated at a temperature of 120 °C, a maximum water absorption of 50%, and a conductivity of at or above 0.1 S/cm for their use as an alternative to the combustion

engine for auto-industry.[15] Efforts are being made to improve PEMs for the purpose of commercialization by improving upon previously discovered membranes like the costly Nafion® and for the design of new cheaper thermo-stable membranes such as polystyrenes, poly(aryl ether)s, poly(aryl ether sulfone)s, and polyimide derivatives.[16] The difficulties and concerns associated with current PEMFCs paved the way for the invention of alternative fuel cell designs incorporating anionic exchange membranes.

1.5 Alkaline Anionic Exchange Membrane Fuel Cells (AAEMFCs)

The exploration of AAEMFCs has gained considerable interest in recent years due to the difficulties associated with PEMFCs' cost, slow electrode-kinetics, high fuel crossover, and carbon monoxide poisoning of platinum based catalysts.[17] AAEMFCs operate similarly to PEMFCs in that they produce electro-chemical energy through the process of converting hydrogen fuel (or alcohols) and oxygen into water as shown in **Figure 2.**

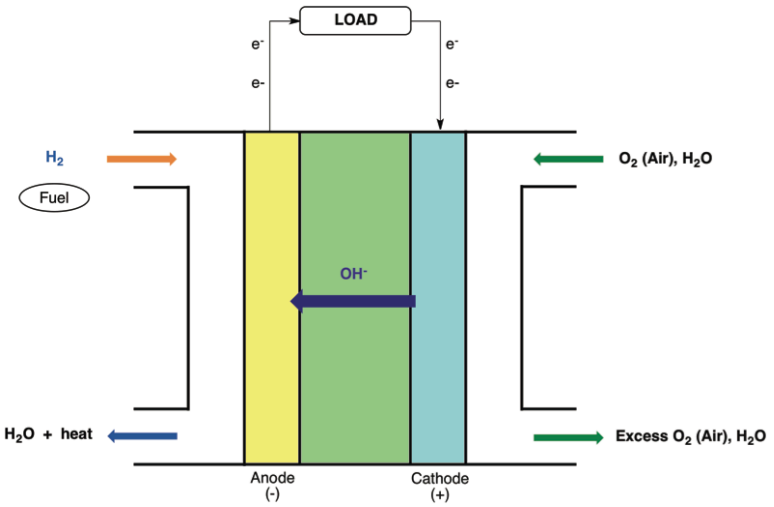

Figure 2. Representation of an AAEMFC

This device example primarily consists of hydrogen fuel, a catalyst anode, a polymer anion exchange membrane, a catalyst cathode, and oxygen (other fuels such as methanol can be used). Oxygen initially is reduced and combined with water and electrons at the cathode, generating hydroxide ions that are diffused through the polymer cationic exchange membrane via hydrophilic micro-channels. The hydroxide ions react with hydrogen to produce water in turn generating electrons that travel by means of the external circuit towards the cathode where they assist in the oxygen reduction process. The half and overall reactions can be observed below.

Anode	$H_2 + 2OH^- \longrightarrow 2H_2O + 2e^-$
Cathode	$^1/_2\, O_2 + H_2O + 2e^- \longrightarrow 2OH^-$
Overall reaction	$H_2 + {}^1/_2\, O_2 \longrightarrow H_2O$

It has been proposed that the diffusion of both protons and hydroxide ions occurs through a Grotthuss like approach. Hydroxide ions are transported through water via the hydrogen-bonded network in a structural mechanistic fashion with the transfer of protons by O – H bond breaking as shown in **Figure 3**. The passage of charge defects in water is a concerted dynamic proton transfer along hydrogen bonds and reorganization of the local environment.[18] Although this is a supported theory by experimental results, there is still skepticism and other theories have gained momentum and it is now believed that a hyper-

coordination mechanism occurs through a fourth hydrogen bond occurring in hydroxide ion diffusion.[19]

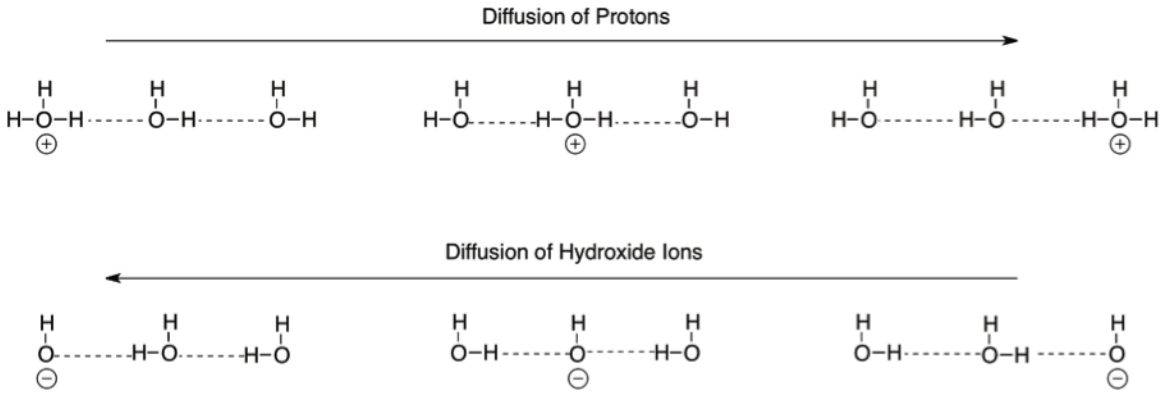

Figure 3. Grotthuss Mechanism for Proton and Hydroxide Ion Diffusion.

The high pH environment that is induced in this system allows for the incorporation of cheaper non-noble catalysts due to the higher reaction efficiency kinetics occurring at the cathode than in PEMFCs due to the high activity of the oxygen reduction reaction.[20, 21] The anionic exchange membrane (AEM) also decreases fuel crossover especially when a methanol source is implemented because hydroxide ions are being transported across the membrane in an opposite direction to the methanol fuel source which prevents a decrease in energy output.[22] It should be noted that methanol is also considered to be a safer fuel for storage and transportation than hydrogen, but one caveat is carbon dioxide is produced as a byproduct.[23] Although AAEMFCs have several

advantages over current PEMFCs, there are still problems plaguing the commercialization of this particular fuel cell with regards to the conducting performance and durability of the anion exchange membrane.

1.6 Challenges for AAEMFCs

Much research has been performed in the development of anion exchange membranes. The AEM consists of a polymer backbone tethered with various types of cationic side groups as shown in **Figure 4** below and will be discussed in more depth later.

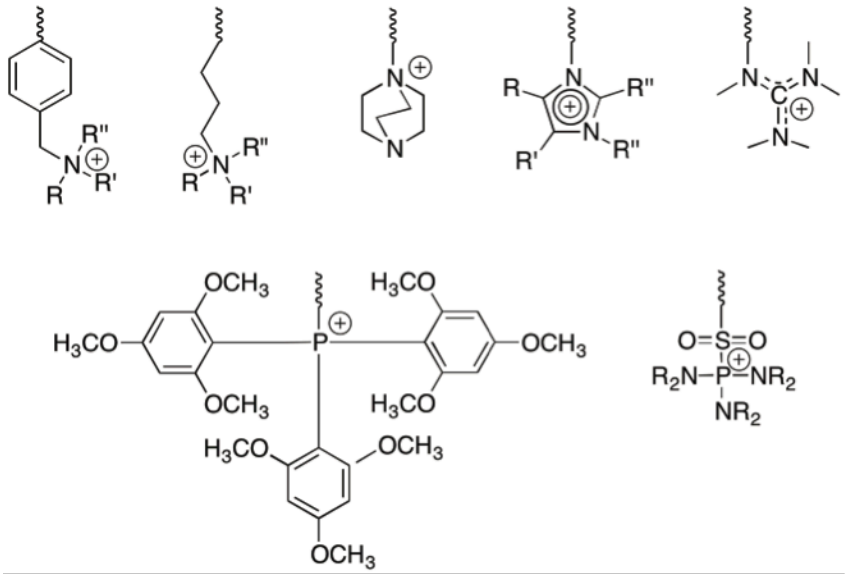

Figure 4. Various Types of Cationic Side Groups in AEMs.

The chief principle of the membrane is to only allow for high conductivity of hydroxide ions from the cathode to the anode and also to prevent electrons or fuel

crossover. It is essential for AEMs to maintain good mechanical properties and be operated at elevated temperatures with minimal degradation or water absorption.[24] But, hydroxide ions are a challenge in fuel cell performance because they are bigger in size and thus exhibit a lower conductivity than protons.[25] The membrane must also be both thermally and chemically stable; however, the relatively high alkaline conditions cause difficulties with regards to the degradation of the polymer backbone and cationic side groups being used in current AEMs. The two major degradation pathways in which hydroxide ions can react are either by a nucleophile displacement or Hoffman β-hydrogen elimination as shown below in **Scheme 1.**[26, 27]

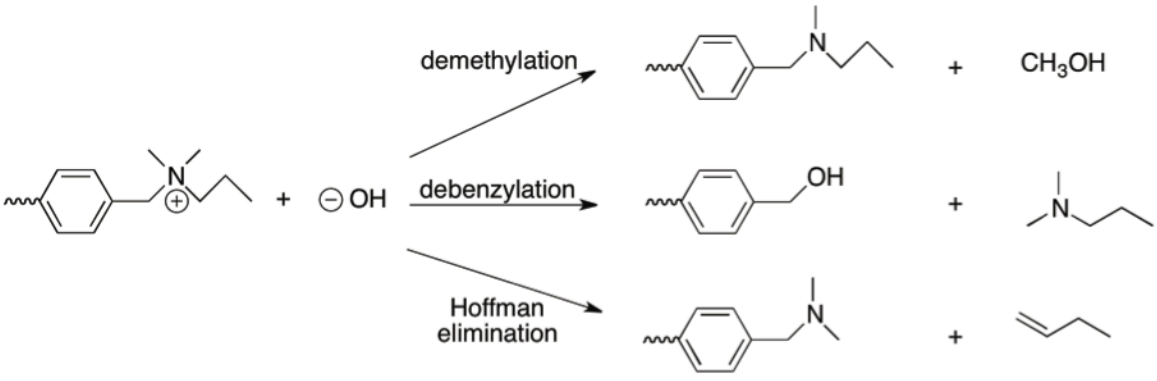

Scheme 1. Nucleophilic Displacement and Hoffman Elimination Side Group Degradation.

Hoffman β-hydrogen elimination is kinetically favored over nucleophile displacement at or below 60 °C and can be entirely avoided if β-hydrogens are completely

removed from the polymer backbone and tethered cationic side groups.[28] New cationic side groups are being explored to improve upon traditional quaternary ammonium moieties that can withstand hydroxide degradation in elevated alkaline temperature conditions with increased hydroxide conductivity. Some of these cationic moieties include; benzyl-trialkylammonium[29], alkyl-side-chain quarternary ammonium groups[30], heterocycle (DABCO) quartenary groups[31], imidazolium groups[32], guaninidium groups[33], quartenary phosphonium groups[34], X-P-N based groups[35], and metal complexes are shown in **Figure 4**.[36] AEMs need to perform at higher temperatures in order to improve electrical efficiency output, and polymers with thermally stable backbones and hydrolytically stable linkages such as poly(aryl ether)s and poly (aryl ether sulfone)s are being investigated as well as co-block and lightly cross-linked polymers to improve hydroxide conductivity and prevent degradation via microphase separation of the backbone and cationic side groups.

1.7 Characterization of AEMs and Importance

Hydroxide ions travel through an anion exchange membrane by diffusing through micro-channels that are filled with water that has penetrated and filled these voids. Water enables the conduction of hydroxide ions from the anode to the cathode. If the membrane has too high of an ionic resistance, water uptake will be low causing the AEM to dry out. Whereas, if the membrane has too low of an ionic resistance, water uptake will be high causing the AEM to flood and reduces the mechanical properties of the membrane due to the stress of dimensional swelling.[37] Both these scenarios diminish the energy output and

affect the overall performance of the AAEMFC. Thus, AEM water uptake is a very important aspect for both hydroxide conductivity and mechanical properties of the membrane. Water uptake (WU) is defined by **Equation 1**, where w_{wet} is the mass of the hydrated membrane and w_{dry} is the mass of a dry membrane form.

$$WU\% = \frac{w_{wet} - w_{dry}}{w_{dry}} \times 100\% \qquad \textbf{Equation 1}$$

Equivalence weight (EW) reflects the mass of the polymer per mole of cationic ionic groups as shown in **Equation 2**.

$$EW = \left(\frac{g}{equiv.}\right) = \frac{MW_{repeat\ unit}\ \left(\frac{g}{mol}\right)}{moles_{cationic\ groups}\ \left(\frac{mol}{equiv.}\right)} \qquad \textbf{Equation 2}$$

Ion exchange capacity (IEC) is the amount of hydroxide ions per gram of dried polymer and is reported in milliequivalents/gram. IEC can be calculated as shown in **Equation 3** or can be determined via titration as shown in **Equation 4** where c is the concentration and V is the volume.

$$IECcalc. = \left(\frac{mequiv.}{g}\right) = \frac{1}{EW\left(\frac{g}{equiv.}\right)} \times 1000 \qquad \textbf{Equation 3}$$

$$IEC_{titr.}\ (\text{mmol/g}) = \frac{c_{NaOH}V_{NaOH} - c_{HCl}V_{HCl}}{m_{dry}} \qquad \textbf{Equation 4}$$

Ion exchange capacity is an important parameter for AEMs because it reflects the hydroxide ion conductivity ability of the membrane. A high IEC usually correlates to better conductivity, but in turn also causes an increase in the water uptake and can be detrimental to the mechanical properties of the membrane affecting the overall performance of the AAEMFC cell. Even though a large IEC value is greatly wanted, water uptake has to be also taken in to consideration. This can be achieved through tailoring the IEC value by incorporating the desired amount of cationic groups present in the membrane while keeping the water uptake as low as possible without compromising the mechanical properties.[38] Thus, an equilibrium between IEC and WU is vital for the success of an AEM that can conduct hydroxide ions at an efficient rate.

While WU, IEC, and conductivity are essential standards for comparison, it is likewise necessary to obtain thermal and chemical properties of AEMS due to operating at high temperatures under alkaline conditions. Thermal data are used to determine the maximum temperature at which a membrane can operate before mechanical properties or chemical degradation compromise the AEM. Thus, all these properties are important when fabricating a prospective anion exchange membrane for use as an AAEMFC.

1.8 Poly(aryl ether sulfone)s (PAES)

Poly(aryl ether sulfone)s are a family of amorphous engineering thermoplastics that have gained considerable interest in recent years for the potential use as the polymer backbone in anion exchange membranes that are required by AAEMFCs. AEMs are

subjected to harsh working conditions and PAES display the desirable physical and chemical characteristics for necessary performance in the basic environment.

In 1965, the Union Carbide company produced the first commercially viable poly(aryl ether sulfone), Udel, which is still globally used today. PAES can be synthesized by two methods: nucleophilic aromatic substitution, NAS, or electrophilic aromatic substitution.[39] The NAS polycondensation approach is currently being used for the commercial production of Udel. This synthesis involves the reaction between a Bisphenol-A sodium salt and 4,4-dichlorophenyl sulfone, at an elevated temperature, to yield Udel. The reaction is performed in the presence of a polar aprotic solvent, such as NMP or DMSO, to aid in the reaction as well as being high boiling organic solvents as shown in **Scheme 2** below.

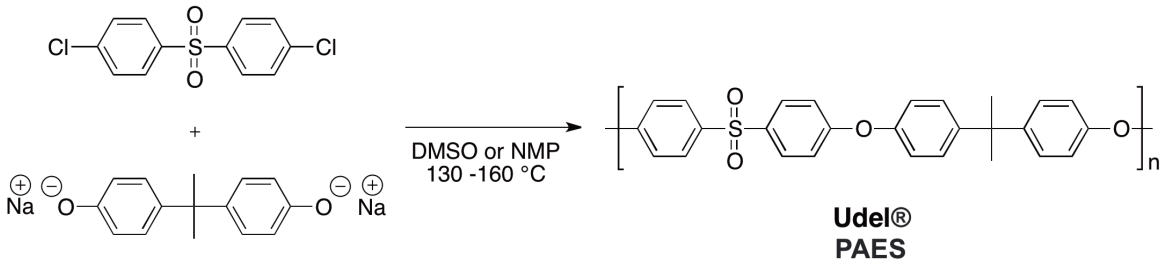

Scheme 2. Synthesis of PAES via NAS.

PAES are mainly composed of an aryl-sulfonyl-aryl repeat unit with ether linkages. Both the polar sulfone subunit and rigid aromatic phenyl regions give rise to

excellent thermal properties. The 5% degradation temperature, $T_{d5\%}$, is the temperature at which a polymer decomposes 5% of its original mass. The glass transition temperature, T_g, is the temperature in which a polymer transitions from a hard glass-like phase to a soft rubber-like phase. PAES have relatively high $T_{d5\%}$ values that exceed 400 C and T_g values that are in excess of 190 °C dependent on the relative structure.[40, 41] Several commercially available PAES with chemical repeat units and T_g values are shown in **Figure 5.**

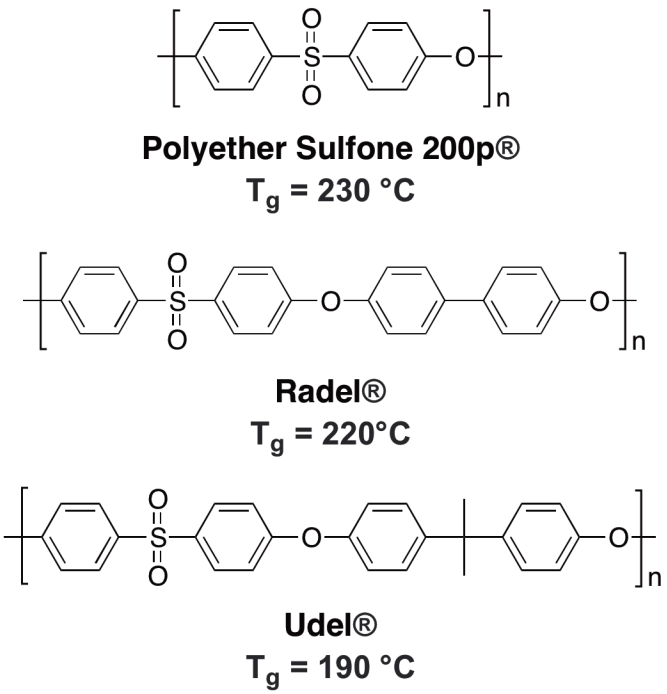

Figure 5. Commercially Available PAES and their respective T_g values.

The relatively high T_g values allow for good mechanical strength while operating at elevated temperatures and also are chemically resistant towards oxidation and

hydrolysis that can occur under alkaline conditions. These qualities make PAES a very suitable candidate as a prospective polymer backbone for use as an AEM.[42]

1.9 Polymerization of PAES via Nucleophilic Aromatic Substitution, NAS

Poly(aryl ether sulfone)s are generally synthesized via a nucleophilic aromatic substitution pathway that occurs through the substitution of an aryl halide leaving group by a nucleophile.[42] The aryl halide group is activated by a strong electron withdrawing group, EWG.

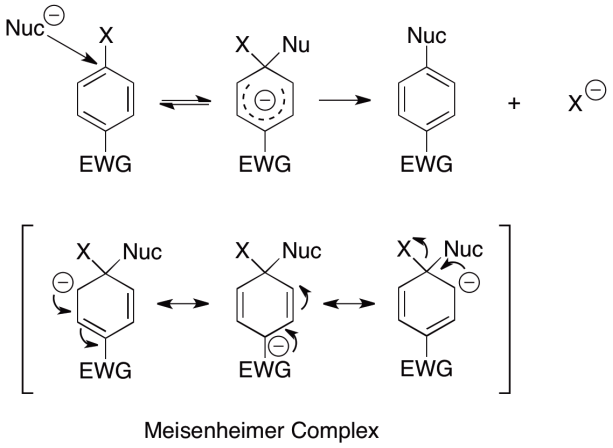

Scheme 3. NAS Mechanism for a *para*-activated System.

The first step in the mechanism occurs when the nucleophile attacks the *ipso* carbon generating a resonance stabilized Meisenheimer complex intermediate. This initial sequence is the rate determining step and also is reversible. The second step involves

aromaticity regeneration of the benzene ring via loss of the halide group and is non-reversible as shown in **Scheme 3.**

PAES are generally synthesized between an A_2 bisphenol monomer and a B_2 diaryl halide sulfone monomer. The aryl halides are usually located in *ortho* and *para* positions, relative to the strong EWG. Activation is a result of the decreased electron at the *ipso* carbon atom. The EWG also stabilized the Meisenheimer complex, which ultimately leads to creating linear polymer chains. However, Kaiti *et al*[43] have recently found that 3,5-*meta* activated diaryl halide systems can undergo NAS polycondensations reactions in which the EWG is in the *meta*-position in regards to the polymer backbone and several different types of EWG have been shown to undergo polymerization as depicted in **Scheme** 4.[44,45,46]

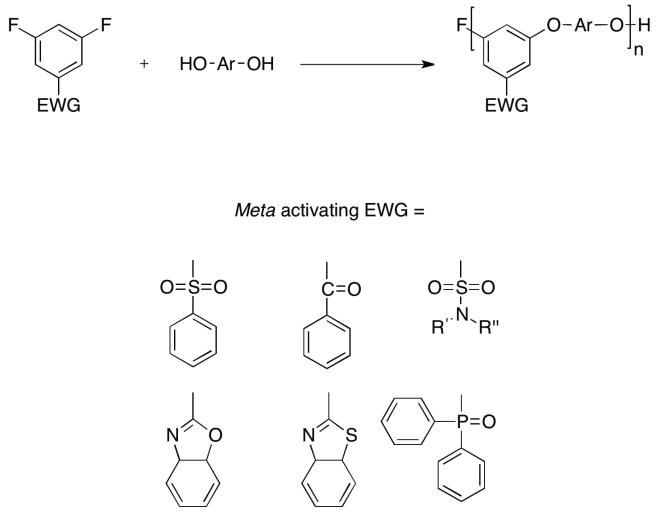

Scheme 4. Synthesis of 3,5-*meta*-activated NAS Systems

The net effect is that the activating group is in a pendent position, relative to the backbone. This allows for the incorporation of various functional groups pendent to the backbone via “pre” or “post” functionalization without affecting the overall physical or chemical properties of the polymer backbone.

1.10 PAES as AEMS and Functional Group incorporation

Cationic groups must be incorporated into PAES for the functional purposes of conducting hydroxide ions required by anion exchange membranes in AAEMFCs. Polymer functionalization can occur through a “pre” or “post” modification route as shown in **Figure 6**.[47]

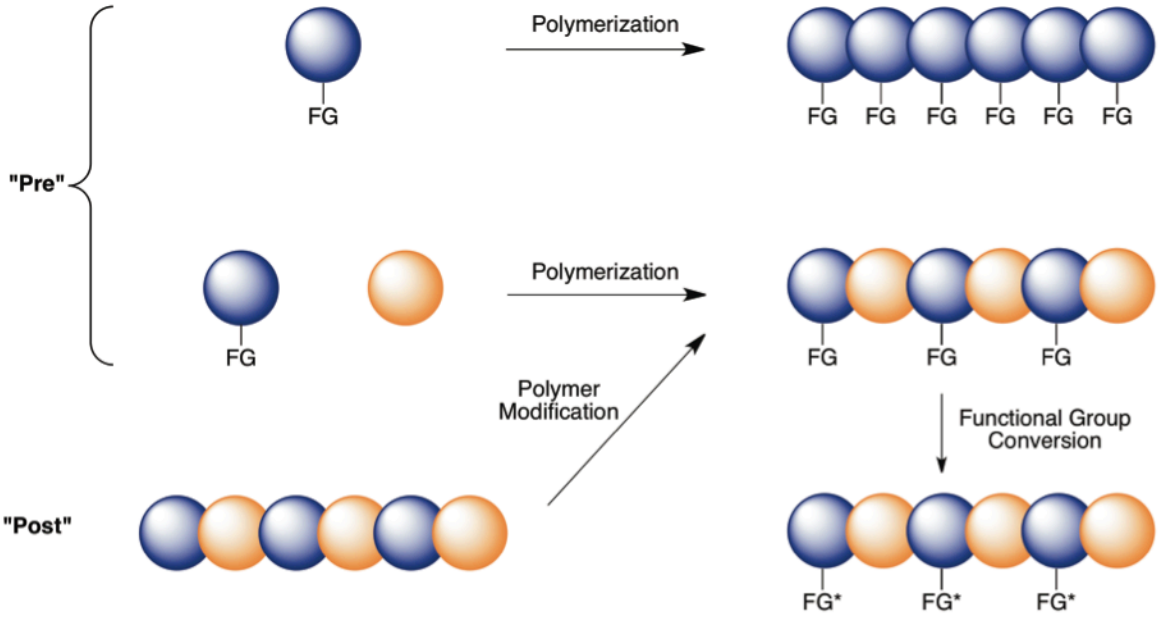

Figure 6. Functionalization of Polymers via “pre” vs. “post” modification.

In pre-modification, monomers contain the desired functional group and are then polymerized. The advantages of "pre" monomer functionalization are being able to control the degree of functionalization and also location of said functional groups. However, the functional group must survive through the polymerization and this becomes a problem with the synthesis of PAES due to the desired cationic functional group not being able to endure the NAS polymerization conditions.

Thus, it is necessary to take a post-modification synthesis route by integrating cationic functional groups after the polymer has been made for practical use as an AEM. Although this allows for cationic functional groups to be present, there are several disadvantages caused by the post functionalization reaction conditions including: the lack of control of functionalization or location, the possibility for side reactions, crosslinking, or even polymer degradation.

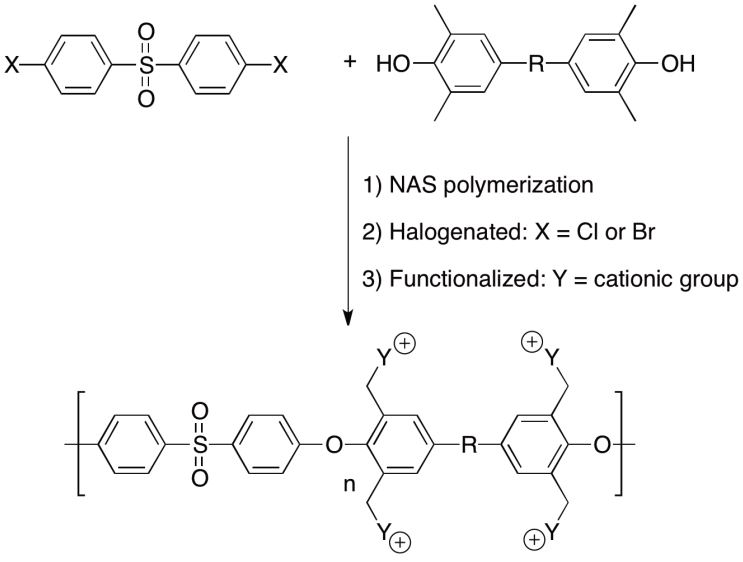

Scheme 5. General Synthesis for PAES used for AEMs.

PAES for use as AEMs are typically made through a post-functionalization route. Typically a bisphenol monomer, with methyl groups, is polymerized with a diaryl sulfone monomer. The polymer is isolated and then the methyl groups are randomly halogenated (chloro or bromo) via a radical mechanism process.[48] Finally, the benzylic halogen groups are substituted with the desired cationic group.

1.11 Current Work

The goal of this project is to improve upon previous PAES that have been researched for their intended use in AAEMFCs. PAES demonstrate all the thermal and chemical properties that are wanted for an anion exchange membrane, but when cationic groups are located directly on the backbone this becomes problematic. These benzylic cationic groups raise the hydrophilicity of PAES backbone and in turn allow for an increase in access towards hydroxide ions. Polar sulfone groups also are electron withdrawing and this enhances the ability for hydroxide atoms to attack and degrade the PAES by a substitution pathway.[49] New methods are being developed with the intention of moving the cationic groups away from the PAES backbone and situating them instead in truly pendent positions. This relocation allows for the PAES to maintain resistance towards hydrolysis and oxidation in addition to preserving excellent thermal properties through microphase separation. This project will achieve these pendent cationic groups by taking advantage of a 3,5-*meta* system as shown in **Figure 7.**

The 3,5- system is a geometric isomer of the traditional 4,4'-diphenyl sulfone. This unique monomer has the ability to produce high molecular weight polymers and similarly allow for the insertion of cationic groups that are situated in truly pendent positions from the PAES backbone. The Fossum Research group has previously shown the advantage of this type of system in relation to PEMFCs where the sulfonic groups were located on the 3,5-*meta* systems. These pendent position displayed a decrease in WU% and an increase in both IEC and proton conductivity, relative to the sulfonic acid groups located directly on the backbone.

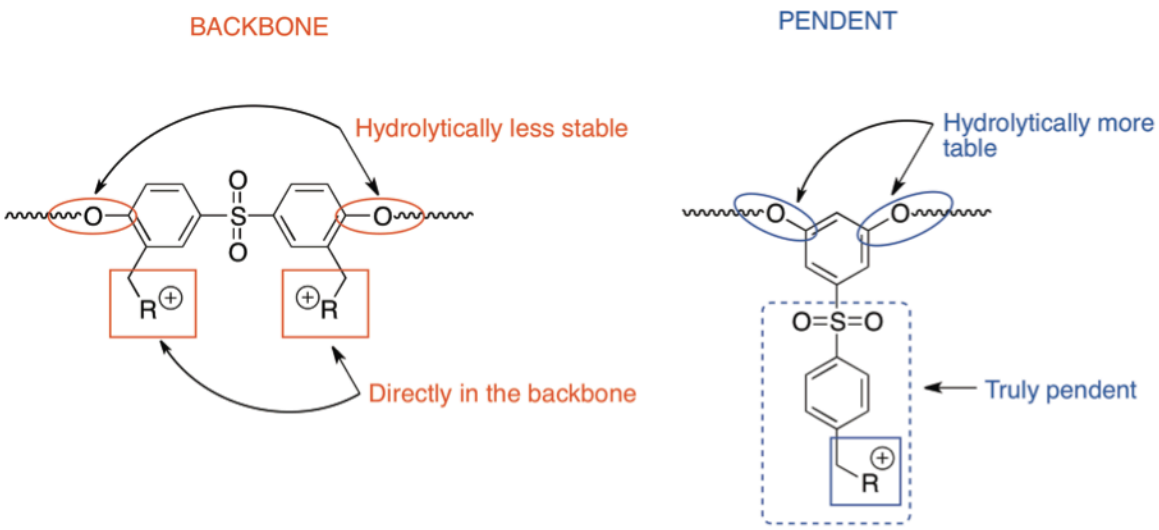

Figure 7. Backbone vs. Pendent Functional Groups

In this project, a series of poly(aryl ether sulfone) copolymers with varying percentages of quaternary ammonium groups will be synthesized and characterized for the

intended use as AEMS. A post-functionalization pathway will be used where the PAES polymers will be made first by a nucleophilic aromatic substitution route where varying percentages of 4,4'-difluordiphenylsulfone and 3,5-difluoro-4'-methyldiphenylsulfone will react with Bisphenol-A. The tolyl groups will then be brominated via a radical bromination process and, finally, will be functionalized with three different quarternary ammonium groups: 1-methylimidazole, trimethylamine, and *N,N*-dimethylhexadecylamine as shown in **Scheme 6.**

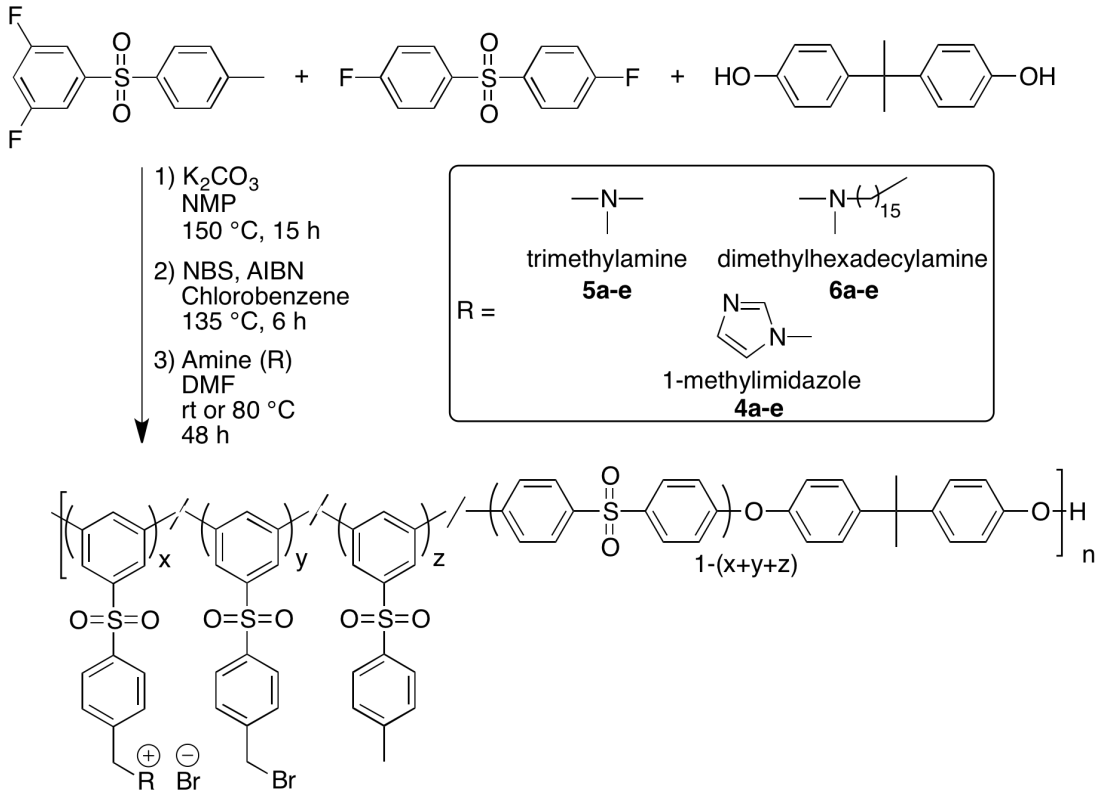

Scheme 6. Synthesis of 3,5-*meta*-activated PAES with Quaternary Amines for AEMs.

The polymers will be tested for WU%, IEC values, and thermal properties in order to see if they demonstrate desirable anion exchange membrane characteristics for AAEMFCs.

2. EXPERIMENTAL

2.1. Instrumentation

Unless otherwise stated, all experiments were performed under a nitrogen atmosphere and all liquid mixtures were transferred via syringes. All ^{1}H and ^{13}C Nuclear Magnetic Resonance (NMR) spectra were acquired on a Bruker AVANCE 300 MHz NMR spectrometer operating at 300 and 75.5 MHz, respectively. All samples were dissolved in chloroform-*d* ($CDCl_3$) or dimethyl sulfoxide-d_6 (DMSO-d_6) at a concentration of (~50 mg/0.7 mL). Size Exclusion Chromatography (SEC) analysis was performed using a system consisting of a Viscotek Model 270 Dual Detector (viscometer and light scattering) and a Viscotek Model VE3580 refractive index detector. Two Jordi Gel Fluorinated DVB MB columns (heated to 35 °C) were used with tetrahydrofuran/ 5% (v/v) acetic acid as the eluent and with a GPC-Max VE-2001 pump operating at 1.0 mL/min. Number average molecular weights, M_n, were determined with the light scattering detector and the dispersity values were determined with the RI signal (calibrated with polystyrene standards). Thermogravimetric Analysis (TGA) and Differential Scanning Calorimetry (DSC) data were obtained by TA Instruments Q500 TGA and Q200 DSC, at a heating rate of 10 °C/min. The glass transition temperature, T_g, and the degradation temperature, T_d, were determined with TA universal analysis software. Melting points were determined on a MEL-TEMP apparatus and are uncorrected. FT-IR analysis was performed using a Thermo Scientific Nicolet 6700 FT-IR spectrometer with OMNIC series software for

analysis. Titrations were performed using a Corning 430 pH meter in conjunction with a Corning "3 in 1 Combo" electrode.

2.2. Materials

N-methylpyrrolidinone (NMP) and *N,N*-dimethylformamide (DMF) were purchased from Sigma Aldrich Chemical Co., dried over CaH_2, and distilled under nitrogen prior to use. Chlorobenzene was purchased from Sigma Aldrich Chemical Co., dried over $CaCl_2$, and distilled under nitrogen prior to use. Anhydrous tetrahydrofuran was purchased from Sigma Aldrich Co. and used as received. Reagent-grade anhydrous potassium carbonate (K_2CO_3) and anhydrous magnesium sulfate ($MgSO_4$) were purchased from Sigma Aldrich Chemical Co. and dried at 130 °C in an oven prior to use. *p*-Toluenesulfonyl chloride was purchased from Tokyo Chemical Industry Co., recrystallized from hexanes, and dried *in vacuo* prior to use. Bisphenol-A (**1a**) was purchased from Sigma Aldrich Chemical Co., recrystallized from hexanes, and dried *in vacuo* prior to use. 4,4'-Difluorophenylsulfone (**1b**) was purchased from Oakwood Chemical Co., recrystallized from ethanol, and dried *in vacuo* prior to use. 1-Bromo-3,5-difluorobenzene was purchased from Oakwood Chemical Co. and used as received. Reagent grade *N*-bromosuccinimide (NBS), azobisisobutyronitrile (AIBN), trimethylamine solution 45% wt. in H_2O (TMA), *N,N*-dimethylhexadecylamine 98% (DMHDA), 1-methylimidazole reagent grade 99% (1-MI) were purchased from Sigma Aldrich Chemical Co. and used as received.

2.3. Synthesis of 3,5-difluoro-4'-methyldiphenylsulfone (1c)

To a 100 mL round-bottomed flask, equipped with a stir bar, Claisen-adapter, addition funnel, condenser, and gas outlet, were added magnesium turnings 1.35 g (55.8 mmol) submerged in just enough anhydrous tetrahydrofuran (THF) to cover the metal. A mixture of 1-bromo-3,5-difluorobenzene 10.0 g (51.9 mmol) and THF (31.2 mL) was added drop-wise over 20 min to the reaction stirring vigorously at room temperature and continued for an additional 4 h. The reaction was then transferred to an addition funnel for the next step.

To a 100 mL round-bottomed flask, equipped with a stir bar, Claisen-adapter, addition funnel, condenser, and gas outlet, were added *p*-toluenesulfonyl chloride 9.30 g (48.8 mmol) and THF (42.5 mL). The solution from step 1 was added drop-wise to the reaction vessel over 15 min at 0 °C. The reaction continued slowly warming from 0 °C to rt, followed by heating to reflux for an additional 2 h. The reaction mixture was diluted with 200 mL of diethyl ether and transferred to a separatory funnel. The organic layer was washed with dilute HCl (3 x 100 mL), deionized H_2O (3 x 100 mL), 5% $NaHCO_3$ (3 x 100 mL), deionized H_2O (3 x 100mL), and 20% brine solution (3 x 100 mL). The ether layer was isolated and a mixture of deionized H_2O (200mL)/toluene (200 mL) was added to the organic layer and was heated to 80 °C and stirred vigorously for 2 h to remove any excess *p*-toluenesulfonyl chloride. The organic layer was isolated, dried over $MgSO_4$, filtered and vacuum dried to afford a light yellow solid. The product was recrystallized from hexanes

and vacuum dried to afford a white solid (8.01 g, 61% yield, m.p., 117 °C, reference m.p.= 112-113 °C[51]) of 3,5-difluoro-4'-methyldiphenylsulfone. ^{1}H NMR ($CDCl_3$): 2.43 (s, 3H), 6.99 (tt, 1H), 7.35 (d, 2H), 7.47 (m, 2H), 7.84 (d, 2H). ^{13}C NMR ($CDCl_3$): 21.6 (s), 108.6 (t), 111.0 (dd), 128.0 (s), 130.2 (s), 137.2 (s), 145.1 (s), 145.5 (t), 162.8 (dd).

2.4. Representative Procedure for Synthesis of PAES Polymers 2a-e

To a 50 mL round-bottomed flask, equipped with a stir bar, reflux condenser, and nitrogen inlet, were added bisphenol-A, **1a**, (3.00 g, 13.1 mmol), 4,4'-difluorodiphenyl sulfone, **1b**, (3.01 g, 11.8 mmol), 3,5-difluoro-4'-methyldiphenylsulfone, **1c**, (0.356 g, 1.30 mmol), K_2CO_3 (5.45 g, 39.4 mmol), and NMP (20.5 mL). The reaction vessel was immersed into a preheated oil bath and vigorously stirred at 150 °C for 15 h. The reaction was diluted with NMP (10 mL) and added drop-wise into acidified, deionized water (1800 mL) stirring vigorously. The resulting white polymer was collected via vacuum filtration and again added to deionized water stirring vigorously at 80 °C for 4 h to remove excess salts and NMP. The white polymer was collected via vacuum filtration and dried under vacuum for 48 h at 135 °C. The polymer was dissolved in THF (20 mL), precipitated from methanol (500 mL), and collected via vacuum filtration and dried under vacuum for 48 h at 135 °C to afford 4.96 g (88 % yield) of white polymer, **2a**. ^{1}H NMR ($CDCl_3$, δ): 1.72 (s, 6 H), 2.42 (s, 0.3 H), 6.79 (t, 0.1H), 6.93 (d, 4H), 7.03 (d, 3.6H), 7.22-7.28 (m, 0.2H, Ar), 7.22-7.28 (m, 0.2H, Ar), 7.27 (d, 4H), 7.77 (d, 0.2H), 7.88 (d, 3.6 H). ^{13}C NMR ($CDCl_3$,

δ): 21.6, 31.0, 42.4, 111.0, 112.2, 117.7, 119.1, 119.8, 127.8, 128.4, 129.7, 130.0, 135.4, 138.0, 144.4, 144.5, 146.8, 147.2, 152.9, 153.3, 159.5, 162.0.

All subsequent polymerizations were performed under the same conditions with varying percentages of monomers **1b** and **1c** and worked up to obtain polymers **2b**, **2c**, **2d**, **2e**.

(2b) (Monomer: 75% **1b** and 25% **1c** to afford 4.98 g, 85% yield, of white polymer): ^{1}H NMR ($CDCl_3$, δ): 1.72 (s, 6H), 2.42 (s, 0.75H), 6.79 (t, 0.25H), 6.93 (d, 4H), 7.03 (d, 3H), 7.23-7.29 (m, 0.5H, Ar), 7.23-7.29 (m, 0.5H, Ar), 7.27 (d, 4H), 7.77 (d, 0.5H), 7.88 (d, 3H). ^{13}C NMR ($CDCl_3$, δ): 21.6, 31.0, 42.4, 111.0, 112.2, 117.7, 119.1, 119.8, 127.8, 128.4, 129.7, 130.0, 135.4, 138.0, 144.4, 144.5, 146.8, 147.2, 152.9, 153.3, 159.5, 162.0.

(2c) (Monomer: 50% **1b** and 50% **1c** to afford 4.73 g, 80% yield, of white polymer): ^{1}H NMR ($CDCl_3$, δ): 1.72 (s, 6H), 2.42 (s, 1.5H), 6.79 (t, 0.5H), 6.93 (d, 4.0H), 7.03 (d, 2.0H), 7.22-7.31 (m, 1H, Ar), 7.22-7.31 (m, 1H, Ar), 7.27 (d, 4H), 7.77 (d, 1H), 7.88 (d, 2.0H). ^{13}C NMR ($CDCl_3$, δ): 21.6, 31.0, 42.4, 111.0, 112.2, 117.7, 119.1, 119.8, 127.8, 128.4, 129.7, 130.0, 135.4, 138.0, 144.4, 144.5, 146.8, 147.2, 152.9, 153.3, 159.5, 162.0.

(2d) (Monomer: 10% **1b** and 90% **1c** to afford 4.84 g, 81% yield, of white polymer): ^{1}H NMR ($CDCl_3$, δ): 1.72 (s, 6H), 2.42 (s, 2.7H), 6.79 (t, 0.9H), 6.94 (d, 4H), 7.03 (d, 0.4H), 7.23-7.31 (m, 1.8H, Ar), 7.23-7.31 (m, 1.8H, Ar), 7.27 (d, 4H), 7.77 (d, 1.8H), 7.88 (d, 0.4

H). ^{13}C NMR ($CDCl_3$, δ): 21.6, 31.0, 42.4, 111.0, 112.1, 117.7, 119.1, 119.8, 127.8, 128.4, 129.7, 130.0, 135.4, 138.0, 144.4, 144.5, 146.8, 147.2, 152.8, 153.3, 159.5, 162.0.

(2e) (Monomer: 100% **1b** and 0% **1c** to afford 4.61g, 77% yield, of white polymer): ^{1}H NMR ($CDCl_3$, δ): 1.72 (s, 6H), 2.42 (s, 3H), 6.79 (t, 1H), 6.94 (d, 4H), 7.22-7.30 (m, 2H, Ar), 7.22-7.30 (m, 2H, Ar), 7.24 (d, 4H), 7.76 (d, 2H). ^{13}C NMR ($CDCl_3$, δ): 21.6, 31.0, 42.4, 111.0, 112.2, 119.1, 127.8, 128.4, 130.0, 138.1, 144.4, 144.5, 146.8l, 153.3, 159.5.

2.5. Representative Procedure for Bromination of Polymers, 3a-e

To a 50-mL Schlenk flask, equipped with a stir bar, reflux condenser, and nitrogen inlet were added polymer (**2a**) (4.00 g, 9.01 mmol), *N*-bromosuccinimide (0.160 g, 0.901 mmol), a catalytic amount of 2,2'-azobis(2-methylpropionitrile) (0.0148 g, 0.00901 mmol), and chlorobenzene (20 mL). The reaction vessel was sparged by nitrogen for 20 minutes and then immersed into an oil bath and heated to 135 °C for 6 h while being vigorously stirred. The reaction was diluted with chloroform (10 mL) and added drop-wise into stirring ethanol (500 mL). The resulting white polymer was collected via vacuum filtration and dried under vacuum for 5 h at 85 °C. The polymer was dissolved in chloroform (20 mL), precipitated from ethanol (500 mL), collected via vacuum filtration, and dried under vacuum for 24 h at 85 °C to afford 3.46 g (86% yield) of **3a** with 39% bromination of tolyl groups (acquired by ^{1}H NMR integration). ^{1}H NMR ($CDCl_3$, δ): 1.72 (s, 6H), 2.42 (s, 0.23H), 4.49 (s, 0.07H), 6.78 (t, 0.07H), 6.80 (t, 0.03H), 6.93 (d, 4H), 7.03

(d, 3.6H), 7.24-7.30 (m, 0.08H, Ar), 7.24-7.30 (m, 0.12H, Ar), 7.24-7.30 (m, 0.12H, Ar), 7.27 (d, 4H), 7.56 (d, 0.08H), 7.76 (d, 0.12H), 7.81-7.86 (m, 0.08H, Ar), 7.87 (d, 3.6H). ^{13}C NMR ($CDCl_3$, δ): 21.6, 31.0, 31.4, 42.4, 111.0, 111.1, 112.1, 112.4, 117.7, 119.1, 119.8, 127.8, 128.3, 128.4, 128.5, 129.7, 129.9, 130.0, 135.4, 138.0, 140.9, 143.4, 143.7, 144.4, 144.5, 146.8, 146.9, 147.2, 152.8, 153.2, 153.3, 159.4, 159.5, 162.0

All subsequent brominations were performed under the same conditions and work up afforded polymers **3b**, **3c**, **3d**, **3e**.

(3b) (Polymer **2b** with 58% bromination of tolyl (acquired by ^{1}H NMR integration) to afford 3.44 g, 84% yield, of polymer): ^{1}H NMR ($CDCl_3$, δ): 1.72 (s, 6 H), 2.42 (s, 0.34H), 4.49 (s, 0.29H), 6.78 (t, 0.11H), 6.80 (t, 0.14H), 6.93 (d, 4H), 7.03 (d, 3H), 7.24-7.30 (m, 0.29H, Ar), 7.24-7.30 (m, 0.21H, Ar), 7.24-7.30 (m, 0.21H, Ar), 7.27 (d, 4H), 7.56 (d, 0.29H), 7.76 (d, 0.21H), 7.81-7.86 (m, 0.29H, Ar), 7.87 (d, 3H). ^{13}C NMR ($CDCl_3$, δ): 21.6, 31.0, 31.4, 42.4, 111.0, 111.1, 112.1, 112.4, 117.7, 119.1, 119.8, 127.8, 128.2, 128.4, 128.5, 129.7, 129.9, 130.0, 135.4, 138.0, 140.9, 143.4, 143.7, 144.4, 144.5, 146.8, 146.9, 147.2, 152.9, 153.2, 153.3, 159.4, 159.5, 162.0

(3c) (Polymer **2c** with 60% bromination of tolyl groups (acquired by ^{1}H NMR integration) to afford 3.37 g, 80% yield, of polymer): ^{1}H NMR ($CDCl_3$, δ): 1.72 (s, 6H), 2.41 (s, 0.6H), 4.49 (s, 0.6H), 6.79 (t, 0.2H), 6.81 (m, 0.3H), 6.93 (d, 4H), 7.03 (d, 2H), 7.22-7.29 (m, 0.6H, Ar), 7.22-7.29 (m, 0.4H, Ar), 7.22-7.29 (m, 0.4H, Ar), 7.25 (d, 4H), 7.56 (d, 0.6H), 7.76 (d, 0.4H), 7.84 (d, 0.6H, Ar), 7.86 (d, 2H). ^{13}C NMR ($CDCl_3$, δ): 21.6, 31.0, 31.3,

42.4, 111.0, 111.1, 112.1, 112.3, 117.7, 119.1, 119.8, 127.8, 128.2, 128.4, 128.5, 129.7, 129.9, 130.0, 135.4, 138.0, 140.9, 143.5, 143.7, 144.4, 144.5, 146.8, 146.9, 147.2, 152.8, 153.2, 153.3, 159.5, 159.6, 162.0

(3d) (Polymer **2d** with 64% bromination of tolyl groups (acquired by ^{1}H NMR integration) to afford 3.48 g, 79% yield, of polymer): ^{1}H NMR ($CDCl_3$, δ): 1.72 (s, 6.0H), 2.42 (s, 1.0H), 4.47 (s, 1H), 6.78 (t, 0.32H), 6.79 (t, 0.58H), 6.93 (d, 4H), 7.03 (d, 0.4H), 7.23-7.30 (m, 1.15H, Ar), 7.23-7.30 (m, 0.65H, Ar), 7.23-7.30 (m, 0.65H, Ar), 7.25 (d, 4H), 7.56 (d, 1.15H), 7.76 (d, 0.6H), 7.84 (d, 1.15H), 7.88 (d, 0.4H). ^{13}C NMR ($CDCl_3$, δ): 21.6, 31.0, 31.3, 42.4, 110.9, 111.0, 112.1, 112.3, 117.7, 119.1, 119.8, 127.8, 128.2, 128.4, 128.5, 129.7, 129.9, 130.0, 135.4, 138.0, 140.9, 143.5, 143.7, 144.4, 144.5, 146.8, 146.9, 147.2, 152.8, 153.2, 153.3, 159.5, 159.6, 162.0

(3e) (Polymer **2e** with 57% bromination of tolyl groups (acquired by ^{1}H NMR integration) to afford 3.29 g, 75% yield, of polymer): ^{1}H NMR ($CDCl_3$, δ): 1.72 (s, 6 H), 2.42 (s, 1.30 H), 4.49 (s, 1.1H), 6.79 (t, 0.43H), 6.82 (t, 0.57H), 6.94 (d, 4H), 7.23-7.31 (m, 0.86H, Ar), 7.23-7.31 (m, 1.14H, Ar), 7.23-7.31 (m, 0.86H, Ar), 7.26 (d, 4H), 7.50 (d, 1.14H), 7.76 (d, 0.86H), 7.87 (d, 1.14H, Ar). ^{13}C NMR ($CDCl_3$, δ): 21.6, 31.0, 31.3, 42.4, 111.0, 111.1, 112.1, 112.3, 119.1, 119.2, 127.8, 128.2, 128.4, 128.5, 129.9, 130.0, 138.0, 140.9, 143.4, 143.7, 144.4, 144.5, 146.8, 146.9, 153.2, 153.3, 159.5, 159.6.

2.6. Representative Procedure for Amination of Polymers, 4a-e by 1-MI

To a 10-mL round bottom flask equipped with a stir bar, condenser, and gas inlet were added polymer **(3a)** (0.400 g, 0.875 mmol), 1-methylimidazole (0.0288 g, 0.351 mmol), and DMF (4 mL). The reaction vessel was immersed into a preheated oil bath and vigorously stirred at 80 °C for 48 h. The reaction was diluted with DMF (2 mL) and added drop-wise into stirring ethyl acetate (70 mL). The resulting polymer was collected via vacuum filtration and added to stirring acetone (300 mL) for 0.5 h to remove excess starting reactants. The polymer was collected via vacuum filtration and dried under vacuum at 80 °C for 48 h to afford 0.384 g (95.0% yield) of polymer **4a** with 39% amination of tolyl groups (acquired by ^{1}H NMR integration). ^{1}H NMR (DMSO-d_6, δ): 1.57 (s, 6H), 2.28 (s. 0.13H), 5.52 (s, 0.31H), 6.96-7.94 (m, Ar), 9.20 (s, 0.15H); solvent peaks: 1.16 (t), 1.97 (s), 2.07 (s), 2.50 (sp), 2.72 (s), 2.88 (s), 3.45 (s), 3.69 (s), 4.0 (q), 7.94 (s), 8.30 (s). ^{13}C NMR (DMSO-d_6, δ): 31.1, 118.2, 127.4, 128.8, 130.2, 130.7, 135.5, 147.2, 152.7, 161.8, 162.8; solvent peaks: 14.5, 21.2, 36.2, 39.9, 60.2, 170.8, 207.1. Solvent peaks attributed to acetone, DMF, DMSO, and ethyl acetate.

All subsequent aminations were performed under the same conditions and work up gave polymers **4b**, **4c**, **4d**, **4e**.

(4b) (Polymer **4b** with 58% amination of tolyl groups (acquired by ^{1}H NMR integration) to afford 0.351g, 85% yield, of polymer): ^{1}H NMR (DMSO-d_6, δ): 1.58 (s, 6H), 2.28 (s, 0.21H), 3.84 (m, 0.5H), 5.54 (s, 0.32H), 6.68 (m, 0.13H), 6.68 (m, 0.17H), 6.98 (m, 4H,

Ar), 6.98 (m, 3H, Ar), 7.12-7.38 (m, 4H, Ar), 7.12-7.38 (m, 0.2H, Ar), 7.12-7.38 (m, 0.2H, Ar), 7.12-7.38 (m, 0.3H, Ar), 7.44 (d, 0.3H), 7.62 (d, 0.37H), 7.73 (m, 0.3H), 7.84 (m, 0.25H, Ar), 7.84 (m, 3.0, Ar), 8.0 (d, 0.3H), 9.24 (s, 0.22H); solvent peaks 1.16 (t), 1.97 (s), 2.07 (s), 2.50 (sp), 2.72 (s), 2.88 (s), 3.45 (s), 4.0 (q), 7.94 (s), 8.30 (s). ^{13}C NMR (DMSO-d_6, δ): 21.6, 31.1, 36.9, 42.3, 51.5, 110.7, 111.2, 111.8, 112.1, 118.2, 119.5, 120.1, 122.9, 124.6, 127.4, 127.5, 128.8, 130.0, 130.7, 133.7, 135.5, 137.5, 140.9, 141.5, 144.1, 144.8, 147.0, 147.3, 152.2, 153.1, 159.5, 161.7; solvent peaks: 14.5, 21.2, 30.9, 36.2, 39.9, 60.2, 162.7, 170.8, 207.1. Solvent peaks attributed to acetone, DMF, DMSO, and ethyl acetate.

(4c): (Polymer **4c** with 60% amination of tolyl groups (acquired by ^{1}H NMR integration) to afford 0.401g, 90% yield, of polymer): ^{1}H NMR (DMSO-d_6, δ): 1.60 (s, 6H), 2.30 (s, 0.60H), 3.52 (m, 0.6H), 5.52 (s, 0.52H), 6.71 (m, 0.2H), 6.71 (m, 0.3H), 6.97-7.02 (m, 4H, Ar), 6.97-7.02 (m, 2H, Ar), 7.19-7.34 (m, 4H, Ar), 7.19-7.34 (m, 0.3H, Ar), 7.12-7.34 (m, 0.4H, Ar), 7.19-7.34 (m, 0.4H, Ar), 7.19-7.34 (m, 0.6, Ar), 7.65 (d, 0.6H), 7.78 (d, 0.4H), 7.87 (m, 0.3H, Ar), 7.87 (m, 2.0, Ar), 8.01 (d, 0.6H), 9.32 (s, 0.38H); solvent peaks 1.16 (t), 1.97 (s), 2.07 (s), 2.50 (sp), 2.72 (s), 2.88 (s), 3.45 (s), 3.69 (s), 4.0 (q), 7.94 (s), 8.30 (s). ^{13}C NMR (DMSO-d_6, δ): 21.4, 31.2, 36.4, 42.4, 51.4, 110.7, 111.2, 111.7, 112.0, 118.2, 119.5, 120.1, 122.9, 124.6, 127.5, 128.0, 128.8, 130.0, 130.2, 130.7, 135.5, 137.7, 138.0, 140.8, 141.5, 144.2, 144.8, 145.2 147.0, 147.2, 152.7, 153.1, 159.5, 161.7; solvent

peaks: 30.9, 33.4, 36.2, 39.9, 60.2, 79.6, 121.7, 128.1, 137.6, 162.7. Solvent peaks attributed to acetone, DMF, DMSO, and ethyl acetate.

(4d): (Polymer **4d** with 64% amination of tolyl groups (acquired by ^{1}H NMR integration) to afford 0.381g, 80% yield, of polymer): ^{1}H NMR (DMSO-d_6, δ): 1.61 (s, 6H), 2.30 (s, 0.90H), 3.56 (m, 0.9H), 5.52 (s, 0.88H), 6.71 (m, 0.6H), 6.71 (m, 0.3H), 6.93-6.99 (m, 4H, Ar), 6.93-6.99 (m, 0.4H, Ar), 7.14-7.35 (m, 4H, Ar), 7.14-7.35 (m, 0.7H, Ar), 7.14-7.35 (m, 0.7H, Ar), 7.12-7.38 (m, 0.7H, Ar), 7.12-7.35 (m, 1.1H, Ar), 7.65 (d, 1.1H), 7.75 (d, 0.8H), 7.84 (s, 0.7H, Ar), 7.87 (d, 0.4H), 8.0 (d, 1.1H), 9.32 (s, 0.5H); solvent peaks 1.16 (t), 1.97 (s), 2.07 (s), 2.50 (sp), 2.72 (s), 2.88 (s), 3.65 (s), 3.86 (s), 4.0 (q), 7.94 (s). ^{13}C NMR (DMSO-d_6, δ): 21.5, 31.2, 36.4, 42.4, 51.4, 110.6, 111.1, 111.7, 112.4, 118.2, 119.5, 120.1, 122.9, 124.6, 128.2, 128.8, 130.0, 130.2, 130.7, 135.5, 137.7, 138.0, 140.8, 141.5, 144.2, 144.8, 145.2 147.1, 147.3, 152.8, 153.1, 159.5, 161.7; solvent peaks: 30.9, 33.4, 36.2, 40.0, 60.2, 121.7, 128.1, 137.6, 162.8. Solvent peaks attributed to acetone, DMF, DMSO, and ethylacetate.

(4e): (Polymer **4e** with 57% amination of tolyl groups (acquired by ^{1}H NMR integration) to afford 0.341 g, 75% yield, of polymer): ^{1}H NMR (DMSO-d_6, δ): 1.61 (s, 6H), 2.31 (s, 1.3H), 3.56 (m, 1.7H), 5.52 (s, 1.1H), 6.72 (m, 0.6H), 6.72 (m, 0.4H), 6.99 (m, 4H, Ar), 7.12-7.35 (m, 4H, Ar), 7.12-7.35 (m, 0.6H, Ar), 7.12-7.35 (m, 0.9H, Ar), 7.12-7.35 (m, 0.7H, Ar), 7.12-7.35 (m, 1.1H, Ar), 7.65 (d, 1.2H), 7.75 (d, 1.2H), 7.84 (s, 0.6H, Ar), 8.0 (d, 1.2H), 9.32 (s, 0.6H); solvent peaks: 1.16 (t), 1.97 (s), 2.07 (s), 2.50 (sp), 2.72 (s), 2.88

(s), 3.65 (s), 3.86 (s), 4.0 (q), 7.94 (s). ^{13}C NMR (DMSO-d_6, δ): 21.5, 31.0, 36.4, 42.4, 51.4, 110.6, 111.1, 111.7, 112.0, 119.5, 122.9, 124.6, 128.8, 130.0, 130.7, 137.7, 140.8, 141.5, 144.2, 144.8, 145.2, 147.1, 153.1, 159.5; solvent peaks: 30.9, 33.4, 36.2, 40.0, 60.2, 121.7, 128.1, 137.6, 162.8. Solvent peaks attributed to acetone, DMF, DMSO, and ethyl acetate.

2.7. **Representative Procedures for Amination of Polymers, 5a-e by TMA**

To a 10-mL round bottom flask equipped with a stir bar, condenser, and gas inlet were added polymer **(5a)** (0.400 g, 0.875 mmol), trimethylamine 45% wt in H_2O (0.0207 g, 0.351 mmol), and DMF (4 mL). The reaction vessel was immersed into a preheated oil bath and vigorously stirred at 80 °C for 48 h. The reaction was diluted with DMF (2 mL) and added drop-wise into stirring ethyl acetate (70 mL). The resulting polymer was collected via vacuum filtration and added to stirring acetone (300 mL) for 0.5 h to remove excess starting reactants. The polymer was collected via vacuum filtration and dried under vacuum at 80 °C for 48 h to afford 0.353 g (90% yield) of polymer **5a** with 39% amination of tolyl groups (acquired by ^{1}H NMR integration). ^{1}H NMR ($CDCl_3$, δ): 1.71 (s, 6H), 2.41 (s, 0.22H), 3.35 (s, 0.11H), 5.21 (s, 0.07 H), 6.78 (t, 0.07H), 6.85 (m, 0.03H), 6.96 (d, 4H), 7.02 (d, 3.6H), 7.25-7.37 (m, 0.08H, Ar), 7.25-7.37 (m, 0.12H, Ar), 7.25-7.37 (m, 0.12H, Ar), 7.27 (d, 4H), 7.57 (m, 0.08H, Ar), 7.77-7.88 (m, 0.08H, Ar), 7.77-7.88 (m, 0.12H, Ar), 7.87 (d, 3.6H); solvent peaks: 2.88 (s), 2.96 (s), 8.02. ^{13}C NMR ($CDCl_3$, δ): 21.6, 31.0, 34.6, 42.4, 52.4, 111.1, 111.2, 112.1, 112.5, 117.7, 119.1, 119.4, 119.8, 127.8, 128.4,

129.7, 130.0, 135.4, 137.6, 138.0, 138.8, 141.2, 144.5, 144.6, 146.8, 146.9, 147.2, 153.1, 153.3, 153.8, 159.5, 159.9, 162.0; solvent peaks: 31.4, 36.5, 79.8, 162.5. Solvent peaks attributed to acetone, DMF, DMSO, and ethyl acetate.

The subsequent aminations were performed under the same conditions and work up gave polymers **5b** and **5e**.

(5b): (Polymer **5b** with 58% amination of tolyl groups (acquired by ^{1}H NMR integration) to afford 0.341 g, 75% yield, of polymer): ^{1}H NMR ($CDCl_3$, δ): 1.69 (s, 6H), 2.39 (s, 0.34H), 3.74 (s, 0.6H), 5.80 (s, 0.20 H), 6.76 (m, 0.11H), 6.76 (m, 0.14H), 6.94 (d, 4H), 7.00 (d, 3H), 7.23-7.26 (m, 0.3H, Ar), 7.23-7.26 (m, 0.2H, Ar), 7.23-7.26 (m, 0.2H, Ar), 7.25 (d, 4H), 7.58 (m, 0.29H), 7.74 (d, 0.2H), 7.75-7.86 (m, 0.3H), 7.85 (d, 3H); solvent peaks: 2.88 (s), 2.96 (s), 8.02 (s). ^{13}C NMR ($CDCl_3$, δ): 21.6, 31.0, 33.6, 36.8, 42.4, 51.2, 110.9, 111.0, 112.1, 112.3, 138.0, 117.7, 119.1, 119.2, 119.8, 127.8, 128.5, 129.7, 130.0, 135.4, 137.6, 139.2, 143.2, 144.4, 144.6, 146.8, 146.9, 147.2, 152.7, 153.1, 153.8, 159.5, 159.7, 162.0; solvent peaks: 31.4, 36.5, 79.8, 162.5. Solvent peaks attributed to acetone, DMF, DMSO, and ethyl acetate.

(5e): (Polymer **5e** with 57% amination of tolyl groups (acquired by ^{1}H NMR integration) to afford 0.350 g, 74% yield, of polymer): ^{1}H NMR (DMSO-d_6, δ): 1.58 (s, 6H), 2.28 (s, 1.2H), 3.01 (s, 5.0H), 4.70 (s, 1H), 6.71 (m, 0.57H, Ar), 6.71 (m, 0.43H, Ar), 6.96 (m, 4H), 7.20-7.32 (m, 4H, Ar), 7.20-7.32 (m, 1.1H), 7.20-7.32 (m, 4H, 0.9H), 7.20-7.32 (m, 0.9H, Ar), 7.75 (d, 1.1H), 7.81 (d, 0.9H), 8.07 (d, 1.1H); solvent peaks: 2.50 (s), 2.72 (s),

2.88 (s), 3.3 (s), 3.45 (s), 7.95 (s). ^{13}C NMR (DMSO-d_6, δ): 21.5, 31.0, 42.3, 44.6, 52.5, 54.8, 111.0, 111.3, 111.7, 112.1, 119.5, 128.0, 128.1, 128.8, 130.7, 135.8, 137.6, 142.2, 143.7, 144.7, 144.5, 153.0, 153.1, 159.5, 159.6; solvent peaks: 31.2, 36.3, 40.0, 162.7. Solvent peaks attributed to acetone, DMF, DMSO, and ethyl acetate.

To a 10 dram vial, equipped with a stir bar, were added polymer film **3c** (0.220 g) and enough trimethylamine 45% wt. to fully submerge the film for 48 h stirring at rt. The film was isolated, washed with deionized H_2O, and then submerged in deionized H_2O for 48 h to remove any starting materials. The film was isolated and dried under vacuum for 48 h at 80 °C to afford to afford 0.238 g (99% yield) of polymer **5c** with 60% amination of tolyl groups (acquired by FT-IR). FT-IR spectra: 1500 cm^{-1} C-C aromatic stretching, 2960 C-H alkyl stretching, 3050 cm^{-1} C-H aromatic stretching, 3200-3700 cm^{-1} O-H stretching.

The subsequent amination was performed under the same conditions and worked up to obtain polymer **5d**.

(5d): (Polymer **5d** with 64% amimation of tolyl groups (acquired by FT-IR) to afford 0.250 g, 99% yield, of polymer): FT-IR spectra: 1500 cm^{-1} C-C aromatic stretching, 2960 C-H alkyl stretching, 3050 cm^{-1} C-H aromatic stretching, 3200-3700 cm^{-1} O-H stretching.

2.8. Representative Procedure for Amination of Polymers, 6a-e by DMHDA

To a 10-mL round bottom flask equipped with a stir bar, condenser, and gas inlet were added polymer **(3a)** (0.400 g, 0.875 mmol), *N,N*-dimethylhexadecylamine (0.100 g,

1.22 mmol), and DMF (4 mL). The reaction vessel was immersed into a preheated oil bath and vigorously stirred at 80 °C for 48 h. The reaction was diluted with DMF (2 mL) and added drop-wise into stirring ethyl acetate (70 mL). The resulting polymer was collected via vacuum filtration and added to stirring acetone (300 mL) for 0.5 h to remove excess starting reactants. The polymer was collected via vacuum filtration and dried under vacuum at 80 °C for 48 h to afford 0.384 g (96% yield) with 39% amination of tolyl groups (acquired by ^{1}H NMR integration). ^{1}H NMR ($CDCl_3$, δ): 0.89 (s, 0.12H), 1.26 (s, 1.03H), 1.50 (s, 0.08H), 1.71 (s, 6H), 2.42 (s, 0.21H), 3.19 (s, 0.07H), 3.25 (s, 0.2H), 5.18 (m, 0.07H), 6.77 (m, 0.03H), 6.77 (m, 0.07H), 6.96 (d, 4H), 7.02 (d, 3.6H), 7.24-7.28 (m, 0.08H, Ar), 7.24-7.28 (m, 0.12H, Ar), 7.24-7.28 (m, 0.12H, Ar), 7.26 (d, 4H), 7.52 (m, 0.08H), 7.75 (d, 0.12H), 7.77-7.87 (m, 0.08H, Ar), 7.87 (d, 3.6H); solvent peaks; 2.19, 2.89, 2.97, 8.02. ^{13}C NMR ($CDCl_3$, δ): 14.2, 21.6, 22.7, 29.3, 29.4, 29.6, 31.9, 42.4, 49.3, 110.8, 110.9, 112.1, 112.6, 117.7, 119.0, 119.8, 127.8, 128.4, 128.8, 19.7, 130.0, 135.4, 137.4, 138.0, 138.8, 140.7, 144.4, 144.5, 146.8, 147.2, 152.8, 153.3, 159.4, 159.9, 162.0; solvent peaks: 29.7, 30.7, 36.5, 77.0, 162.5, 206.9. Solvent peaks attributed to acetone, DMF, DMSO, and ethyl acetate.

All subsequent aminations were performed under the same conditions and worked up to obtain polymer **6b**, but polymers **6c-e** were cast straight on to glass after reaction completion due to insolubility issues.

(6b): (Polymer **3b** with 58% amination of tolyl groups (acquired by ^{1}H NMR integration) to afford 0.350 g, 74% yield, of polymer): ^{1}H NMR (DMSO-d_6, δ): 0.77 (s, 0.3H), 0.93-1.3 (m, 3.9H), 1.50 (m, 0.3H), 1.55-1.72 (m, 6H), 2.27 (s, 0.32H), 2.96 (s, 0.3H), 3.25 (m, 0.6H), 4.62 (s, 0.2H), 6.69-7.02 (m, 0.14H, Ar), 6.69-7.02 (m, 0.11H, Ar), 6.69-7.02 (m, 4H, Ar), 6.69-7.02 (m, 3H, Ar), 7.09-7.40 (m, 0.2H, Ar), 7.09-7.40 (m, 0.2H, Ar), 7.09-7.40 (m, 0.3H, Ar), 7.09-7.40 (m, 4H, Ar), 7.62-7.81 (m, 0.2H, Ar), 7.63-8.05 (m, 0.3H, Ar), 7.63-8.05 (m, 0.3H, Ar), 7.63-8.05 (m, 3H, Ar); solvent peaks: 1.97, 2.07, 2.50, 2.72, 2.89, 4.03, 3.45, 7.95. ^{13}C NMR (DMSO-d_6, δ): 14.3, 22.2, 22.5, 29.2, 29.4, 31.2, 30.9, 31.7, 42.3, 49.8, 111.3, 111.5, 112.0, 112.5, 118.2, 119.4, 120.1, 128.3, 130.1, 130.2, 134.9, 134.5, 135.5, 138.3, 142.4, 144.7, 144.8, 147.0, 147.2, 152.7, 153.0, 159.5, 159.6, 161.8; solvent peaks: 14.5, 21.2, 30.6, 30.8, 36.3,40.0, 60.2, 162.8, 206.3. Solvent peaks attributed to acetone, DMF, DMSO, and ethyl acetate.

(6c): (Polymer **3c** with 60% amination of tolyl groups (acquired by FT-IR) to afford 0.350 g, 74% yield, of polymer): FT-IR spectra: 1500 cm^{-1} C-C aromatic stretching, 2960 C-H alkyl stretching, 3050 cm^{-1} C-H aromatic stretching, 3200-3700 ¯O-H stretching.

(6d): (Polymer **3d** with 64% amination of tolyl groups (acquired by FT-IR) to afford 0.350 g, 74% yield, of polymer): FT-IR spectra: 1500 cm^{-1} C-C aromatic stretching, 2960 C-H alkyl stretching, 3050 cm^{-1} C-H aromatic stretching, 3200-3700 ¯O-H stretching.

(6e): (Polymer **3e** with 57% amination of tolyl groups (acquired by FT-IR) to afford 0.350 g, 74% yield, of polymer): FT-IR spectra: 1500 cm^{-1} C-C aromatic stretching, 2960 C-H alkyl stretching, 3050 cm^{-1} C-H aromatic stretching, 3200-3700 ¯O-H stretching.

2.9. Membrane Preparation Procedure

Anionic membranes were prepared by 3 alternative methods due to solubility issues. Method l; polymers **4a-e**, **5a**, **5b**, **5e**, **6a**, **6b**, and **6e**, were dissolved in DMF or chloroform by a 5-10% (w/w). The solutions were filtered via a 0.45 μm nylon syringe filter, cast on to a glass plate, and dried at increasing temperature from rt to 80 °C under vacuum for 24 h. The membranes were then removed by soaking in DI water and submerged in DI water to remove any residual starting materials. Method 2; polymers **5c** and **5d** were prepared as stated in the previous experimental section. Method 3; after amination, polymers **6c** and **6d** were filtered via a 0.45 μm nylon syringe filter, cast on to a glass plate, and dried at increasing temperature from rt to 80 °C under vacuum for 24 h. The membranes were then removed by soaking in DI water and submerged in DI water to remove any residual starting materials. Finally, the membranes were soaked in 1M NaOH to exchange bromine ions with hydroxide ions and subsequently washed with DI water.

2.10. Characterization of Anionic Membrane Films

2.10.1. Typical Procedure for Finding Water Uptake

Water uptakes were determined by drying the anionic exchange membranes at 80 °C under vacuum for 24 h or until a constant mass was reached. Next the membranes were submerged in water at rt for 24 h. The hydrated films were massed after removing excess water via blotting by Kim Wipe technique. The water uptakes were then calculated using **equation 1** and an average of 3 trials was used for the final determination of water uptake values.

2.10.2. Typical Procedure for Finding Ion Exchange Capacity

Experimental ion exchange capacities were determined by titration. The anionic membranes were dried for 24 h or until a constant mass was reached. Next the membranes were submerged in standardized 0.01M HCl (20 mL) and stirred for 24 h. The membranes and acid solution were back-titrated with standardized 0.01M NaOH while taking pH recordings via a Dow Corning pH probe. The titrated endpoints were found by taking the largest maxima in the d(pH) vs dV titration plots. The IECs were then calculated using **equation 4** and an average of 3 trials was used for the final determination of ion exchange capacity values.

3. Results And Discussion

3.1 Outline of the Project

The goal of this project was to develop AEMs and there were 4 main steps that transpired for generating novel PAES with truly pendent aminated tolylsulfonyl groups including: 1) the synthesis and characterization of the 3,5-difluoro-4'-methyldiphenylsulfone monomer, 2) the synthesis and characterization of random PAES copolymers with varying percentages of 3,5-difluoro-4'-methyldiphenylsulfone and 4,4'-difluorophenyl sulfone while holding Bisphenol-A at a constant value, 3) the synthesis and characterization of the brominated pendent tolylsulfonyl groups of the PAES copolymers, and 4) the synthesis and characterization of the aminated pendent tolylsulfonyl groups with different quaternary ammonium groups.

The 3,5-difluoro-4'-methyldiphenylsulfone monomer allows for the post-functionalization of quaternary ammonium groups through a two-step process in which the tolyl group is radically brominated and followed by a nucleophilic substitution of the bromine in the bromo benzyl group via the Menshutkin reaction. The 3,5-difluoro-4'-methyldiphenylsulfone monomer allows for the incorporation of cationic groups to be located in a truly pendent position from the PAES backbone and in turn increases the hydrolytic, oxidative, and thermal stability of the polymer for better performance as an AEM. A series of functionalized poly(aryl ether sulfone)s, based on 3,5-difluoro-4'-methyldiphenylsulfone, with a varying number of quaternary ammonium groups on the

benzylic sulfonyl moiety position were investigated to better understand and characterize the thermal, mechanical, and AEM properties of the PAES copolymers with the intended use for AAEMFCs.

3.2 Synthesis of 3,5-difluoro-4'-methyldiphenylsulfone (1c)

The synthesis of 3,5-difluoro-4'-methyldiphenylsulfone occurred through a nucleophilic substitution reaction via a Grignard mechanism as shown in **Scheme 7**. Commercially available 1-bromo-3,5-difluorobenzene was reacted with pulverized magnesium turnings for 4 h at rt under a nitrogen atmosphere. The resulting Grignard reagent was allowed to react with commercially available *p*-toluenesulfonyl chloride. After a standard workup the product was recrystallized from hexanes to afford a white solid in 61 % yield.

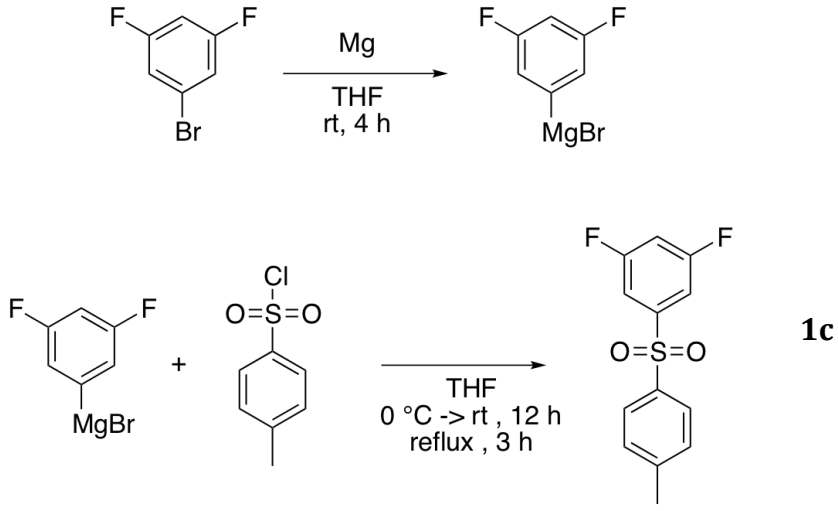

Scheme 7. Synthesis of 3,5-difluoro-4'-methyldiphenylsulfone**, 1c**.

The synthesis of the 3,5-difluoro-4'-methyldiphenylsulfone monomer **1c** was confirmed by ^{1}H and ^{13}C NMR spectroscopic analysis and these spectra can be seen in **Figure 8** and **Figure 9**.

The ^{1}H NMR spectrum of **1c** presents 5 distinct peaks. Proton **a**, the most upfield aromatic proton, occurs as a triplet of triplets at 6.99 ppm due to coupling with the two fluorine atoms with coupling constants ($^{3}J_{H\text{-}F}$= 8.1 Hz) and two protons with coupling constants ($^{4}J_{H\text{-}H}$= 2.2 Hz). Proton **b** occurs as a multiplet at 7.47 ppm due to asymmetric coupling with the two fluorine atoms and the two hydrogen atoms. Proton **c** occurs as a doublet at 7.84 ppm, proton **d** occurs as doublet at 7.35 ppm, and proton **e** occurs as a singlet at 2.43 ppm.

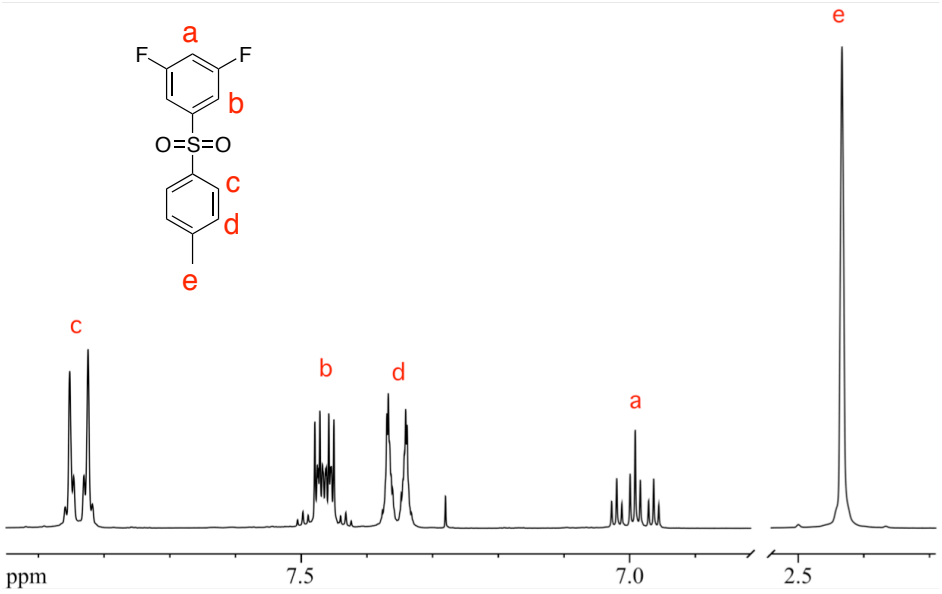

Figure 8: 300 MHz ^{1}H NMR spectrum ($CDCl_3$) of **1c**.

The ^{13}C NMR spectrum of **1c** displays 9 distinct signals. Carbon **a**, the most upfield aromatic carbon, occurs as a triplet at 108.6 ppm, due to coupling with both *ortho* fluorine atoms ($^{3}J_{C\text{-}F}$ = 25.0 Hz). Carbon **b** occurs as a doublet of doublets at 162.8 ppm due to coupling with the *ipso* fluorine ($^{2}J_{C\text{-}F}$ = 255.2 Hz) and the *meta* fluorine ($^{2}J_{C\text{-}F}$ = 11.5 Hz). Carbon **c** occurs as a doublet of doublets at 111.0 ppm due to coupling with the *ortho* fluorine and the *para* fluorine. Carbon **d** occurs as a triplet at 145.5 due to coupling with both *meta* fluorines. All the remaining carbons: **e, f, g, h,** and **i** were identified as singlets and occur at 21.6, 128.0, 130.2, 137.2, and 145.1ppm, respectively.

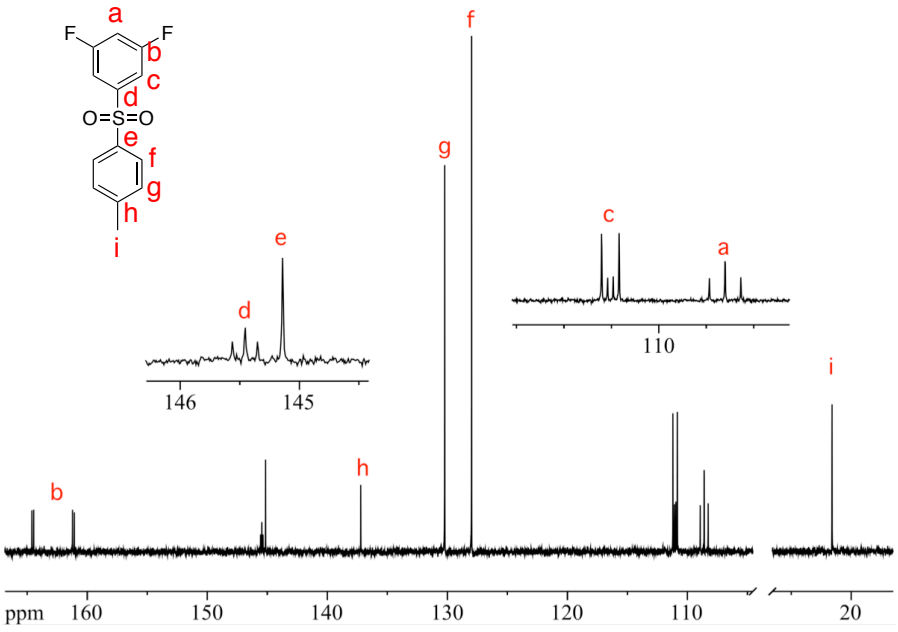

Figure 9: 75.5 MHz ^{13}C NMR spectrum ($CDCl_3$) of **1c**.

3.3. Synthesis of Copolymer PAESs (2a-e) via NAS

A series of poly(aryl ether sulfone)s was synthesized via a typical NAS polycondensation reaction with the following monomers: bisphenol-A, **1a**, 4,4'-difluorodiphenylsulfone, **1b**, and 3,5-difluoro-4'-methyldiphenylsulfone, **1c** as shown in **Scheme 8**.

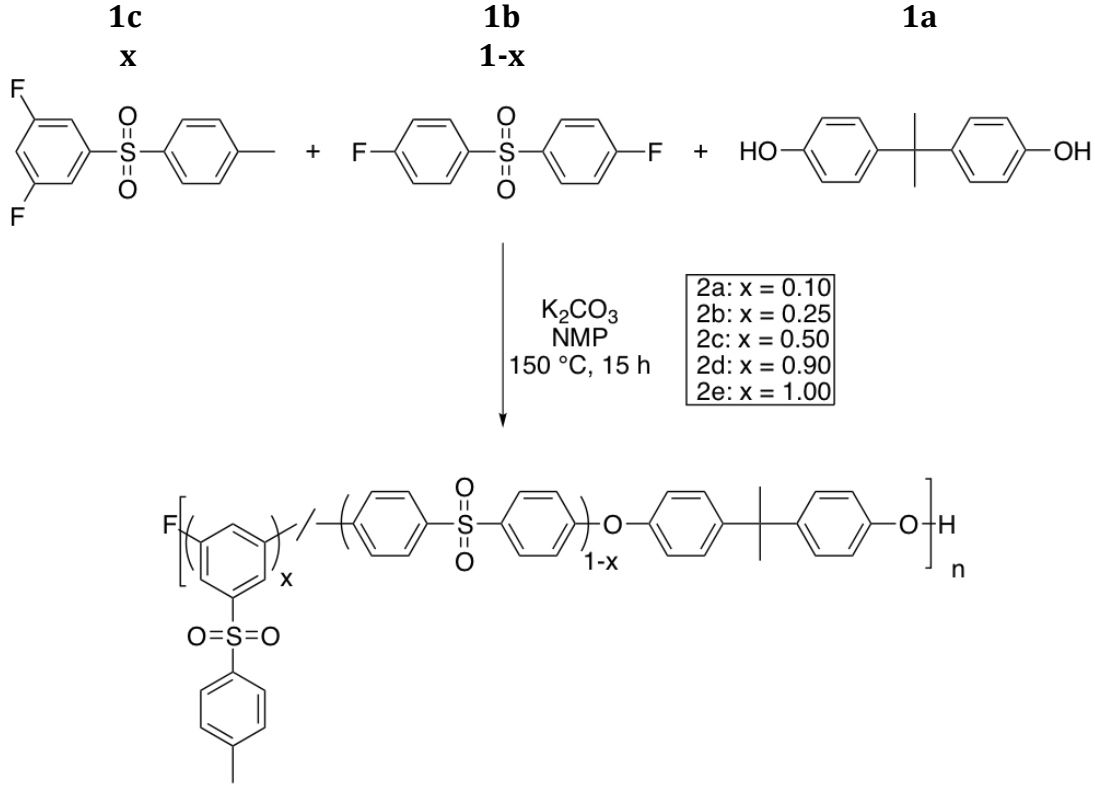

Scheme 8. Synthesis of polymers **2a-e** via NAS.

Monomer **1a** was held at a constant value while varying the molar ratio of monomers **1b** and **1c** with regards to each other (90/10, 75/25, 50/50, 10/90, and 0/100 respectively). The polymerizations were carried out at 150 °C for 15 h. The polymers

were precipitated into acidified DI water and collected by vacuum filtration. The resulting polymers were heated in water at 80 °C for 4 hours to remove any excess salts or NMP. The polymers were then isolated and dried for 48 h at 135 °C. Finally all the polymers were purified by reprecipitation from THF/methanol (solvent/nonsolvent) to remove any cyclic oligomers or impurities to afford polymers **2a-e.**

^{1}H and ^{13}C NMR spectroscopic analyses were used to determine the structure of polymers **2a-e** and an overlay of the ^{1}H NMR and ^{13}C NMR spectra for both polymers **2c** and **2e** is shown in **Figure 10** and **Figure 11**, respectively, to display a comparison and help identify certain peaks.

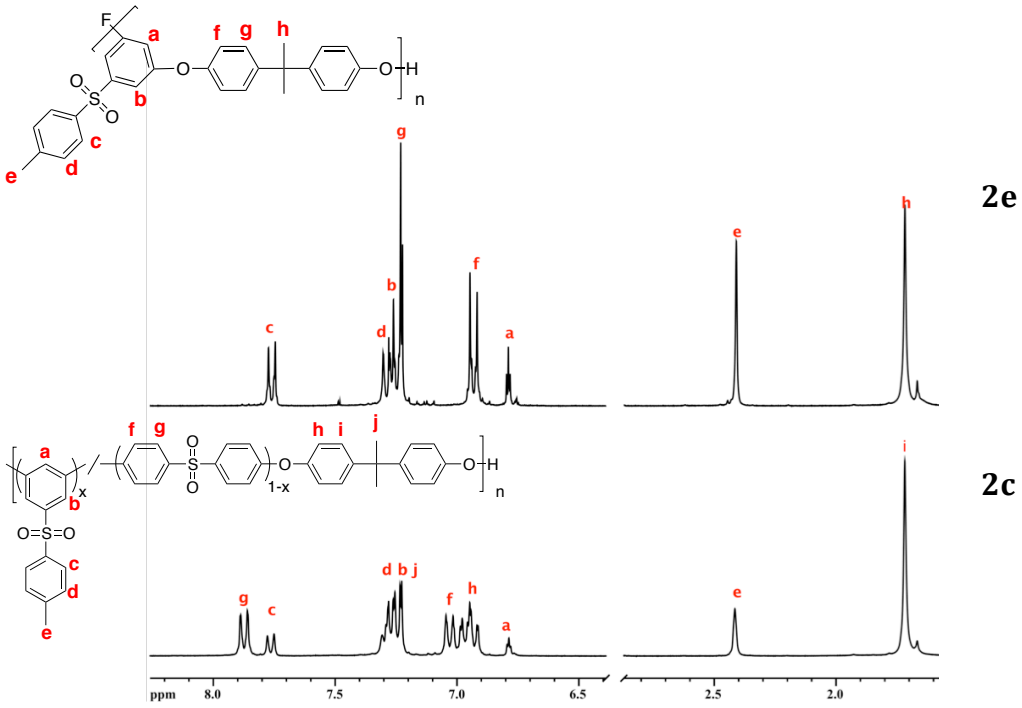

Figure 10. Overlay of 300 MHz ^{1}H NMR spectra ($CDCl_3$) of **2c** and **2e**.

The **2c** ^{1}H NMR spectrum displays 10 distinct peaks, whereas the **2e** spectrum displays 8 distinct peaks, which can be attributed to the lack of presence of monomer **1b.** Proton **a** for both spectra appears as a triplet at 6.79 ppm and demonstrates the displacement of both *meta* fluorines from the original fluorinated monomer with equivalent coupling constants (^{3}J= 2.10 Hz*)*. The mole ratio of bisphenol-A was held constant for both polymers and was used as the standard for integration. The integration of the aromatic protons and non-aromatic protons confirmed that both monomers **1b** and **1c** were equally polymerized with the bisphenol-A monomer for polymer **2c**. Protons **h, j** showed an integration of 6H and proton **e** exhibited an integration of 1.5H and 3H, respectively.

The ^{13}C NMR spectrum of polymer **2c** consists of 23 unique singlet signals and polymer **3e** consists of 15 distinct singlet signals. Carbon atoms **a** and **d**, which were triplets in the monomer appearing at 108.6 and 145.5 ppm, collapsed into singlets at 112.2 and 144.5 ppm. Carbon atoms **b** and **d**, which were doublet of doublets in the monomer occurring at 110.0 and 162.8 ppm, also collapsed into singlets at 159.5 and 111.0 ppm. Both these features confirm the displacement of the *meta*-fluorines. Eight distinct signals appear in the bisphenol-A aromatic region of polymer **2c** due to the influence in connection of either monomers **1b** or **1c**, whereas only 4 distinct signals occur in the same aromatic region of polymer **2e** because it lacks the presence of monomer **1b**.

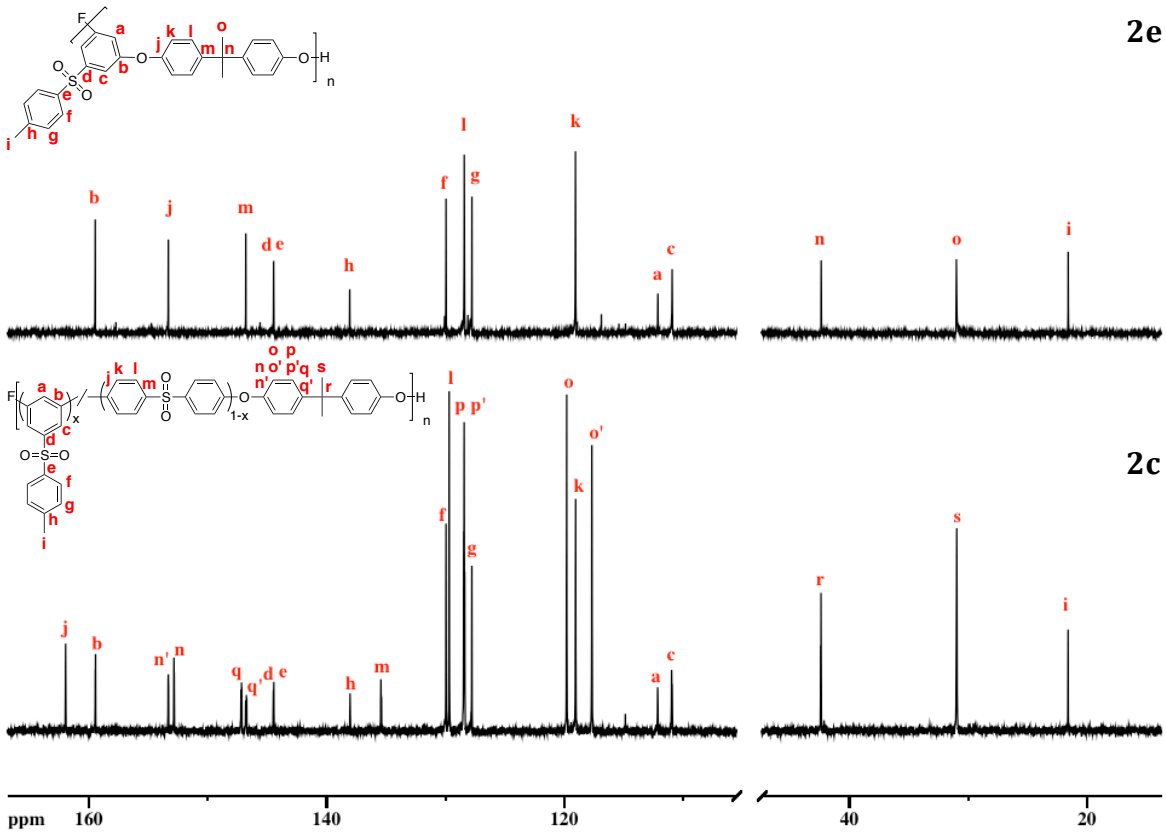

Figure 11. Overlay of 75.5 MHz ^{13}C NMR spectra ($CDCl_3$) of **2c** and **2d**.

Polymers **2a-e** were characterized for their respective molecular weight and thermal data using size exclusion chromatography (SEC), thermogravimetric analysis (TGA), and differential scanning calorimetry (DSC).

Size exclusion chromatography was used to verify the molecular weight (M_w) by using refractive index (RI) with light scattering detectors and was used also to determine

the dispersity (Đ) by using a polystyrene standard calibration. The polymers were dissolved in a THF/ 5% (v/v) acetic acid solution and eluted through the separation columns. Polymers **2a-e** were found to have molecular weights (M_n) between 7000-34,600 Daltons and also a dispersity between 2.6-3.1, which is common for typical NAS polycondensation reactions. The SEC trace of polymer **2c** is shown in **Figure 12** and the molecular weights and dispersity values are found in **Table 1.**

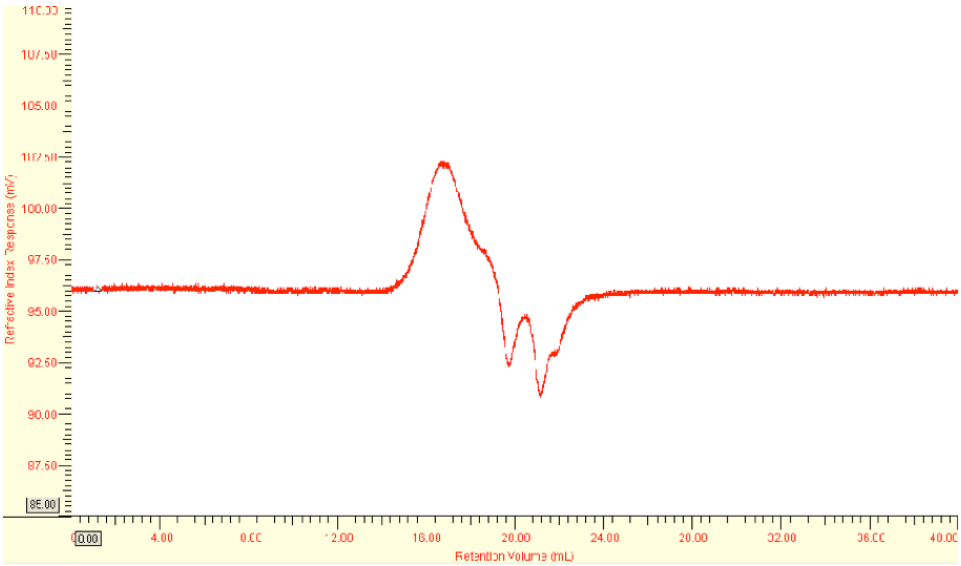

Figure 12. SEC Trace of Polymer **2c**.

Table 1. Molecular Weight and Dispersity Values for Polymers **2a-e**.

Polymer	% Tolyl	M_n (g/mol)	Đ
2a	10	18,600	2.9
2b	25	34,600	2.8
2c	50	29,800	3.1
2d	90	29,200	2.7
2e	100	7,000	2.6

Polymers **2a-d** displayed high enough molecular weights for the casting of practical flexible films, but polymer **2e** was of insufficient molecular weight or too rigid to allow for chain entanglements and ultimately led to a brittle film.

TGA and DSC were both used to determine the thermal properties of polymers **2a-e**. TGA analysis was used to find the 5% degradation temperature ($T_{d5\%}$) of the polymers by heating the polymer under nitrogen and air. As the temperature increases the polymer will reach a point where it begins to degrade and a weight loss is observed. The TGA traces for polymers **2a-e** can be found in **Figure 13** as an overlay.

All of the polymers 2**a-e** exhibited very high thermal stability and were shown to have $T_{d5\%}$ values above 430 °C. T_g values were moderately high and ranged from 132-182 °C and the polymers were completely amorphous. The T_g values decrease as the ratio of monomer **1c** increases with respect to monomer **1b**. The thermal data can be found in **Table 2.**

Table 2. Thermal data for Polymers **2a-e**.

Polymer	$T_{d5\%}$ (°C)	T_g (°C)
2a	472	182
2b	457	176
2c	461	163
2d	420	147
2e	434	134

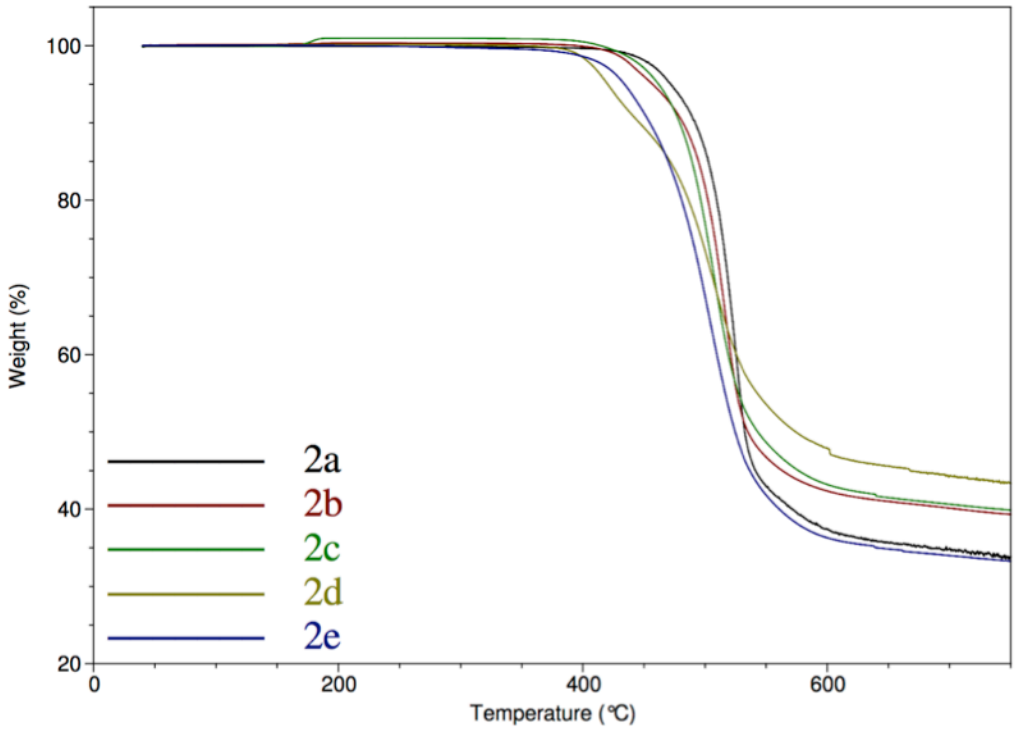

Figure 13. TGA Traces of Polymers **2a-e**.

DSC analysis was used to find the glass transition temperatures (T_g) for the polymers by heating the latter under nitrogen. As the temperature increases the polymer will reach a certain temperature where it transitions from the hard glass like state to a

rubbery like state and this is observed through the heating of a reference sample to match that of the polymer sample. The DSC traces for polymers **2a-e** can be found in **Figure 14** as an overlay.

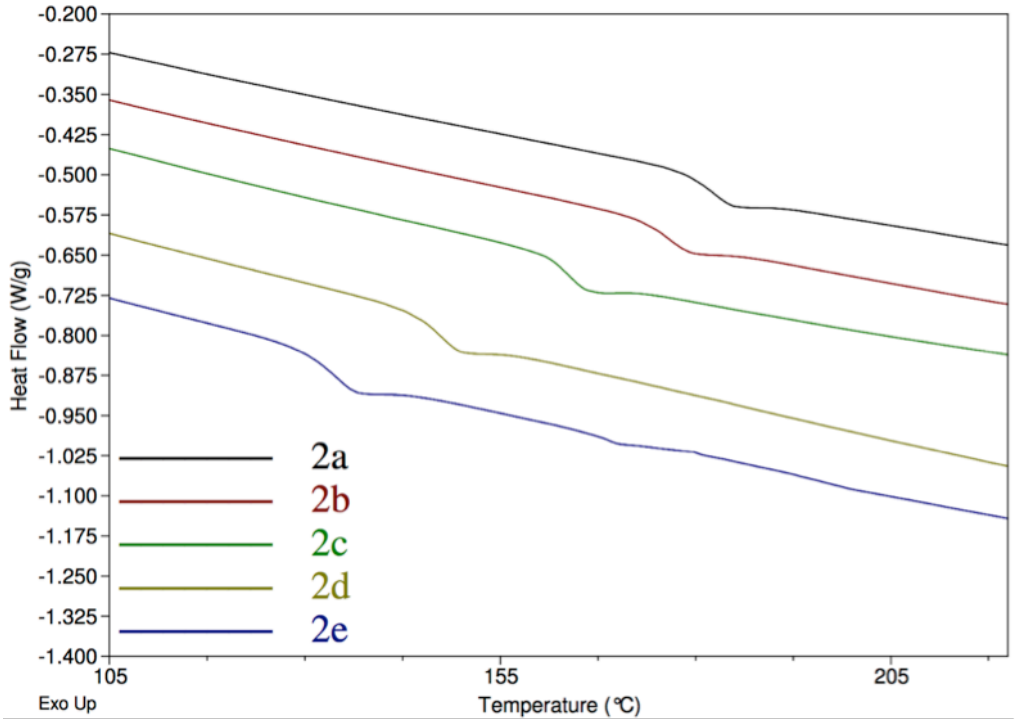

Figure 14. DSC Traces of Polymers **2a-e**.

3.4. Synthesis of Brominated PAES (3a-e)

A series of poly(aryl ether sulfone)s was functionalized by the bromination of the pendent tolylsulfonyl groups via a radical process as shown in **Scheme 9**. Polymers **2a-e** were first dissolved in distilled chlorobenzene and then NBS and a catalytic amount of the radical initiator, AIBN, were added to the systems. All reactions were sparged with

nitrogen and heated to 135 °C for 6 h, after which the polymers were precipitated from ethanol. The polymers were allowed to dry and then reprecipitated from choloroform/ethanol to remove any starting materials or cyclic oligomers. The polymers were then dried at 85 °C for 48 h. NBS was chosen as the brominating agent because it is easier to work with and is safer than bromine itself. The amount of NBS used was in a 1:1 molar ratio to tolyl groups in order to avoid dibromination or other side reactions.

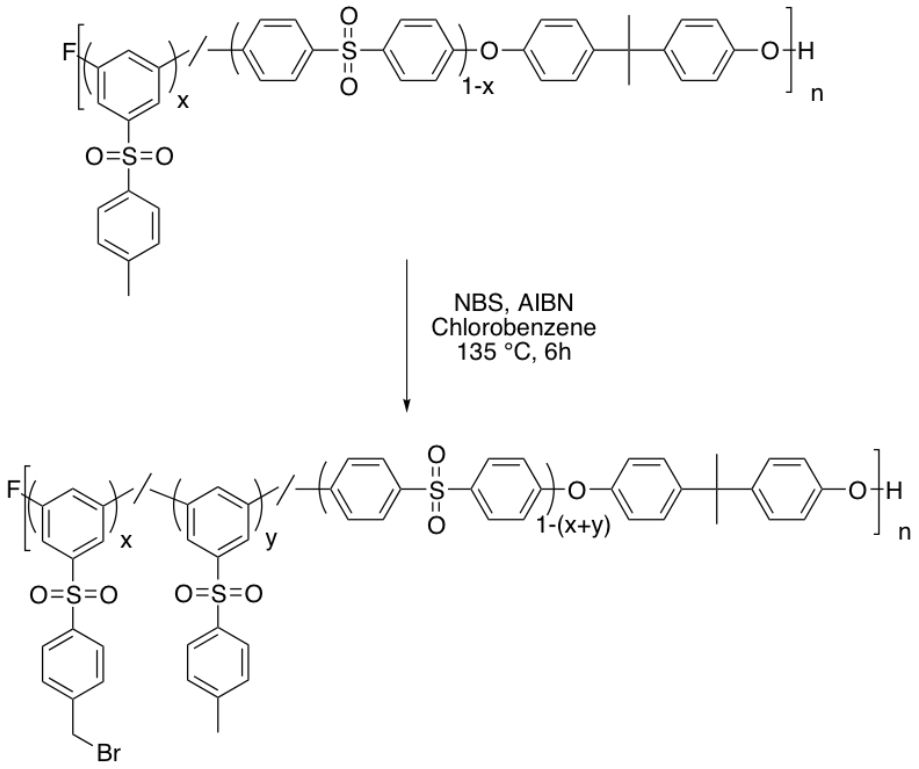

Scheme 9. Synthesis of Polymers **3a-e**, via bromination.

The radical bromination mechanism occurs through generation of benzylic free radicals and results in a chain reaction as shown in **Scheme 10**.

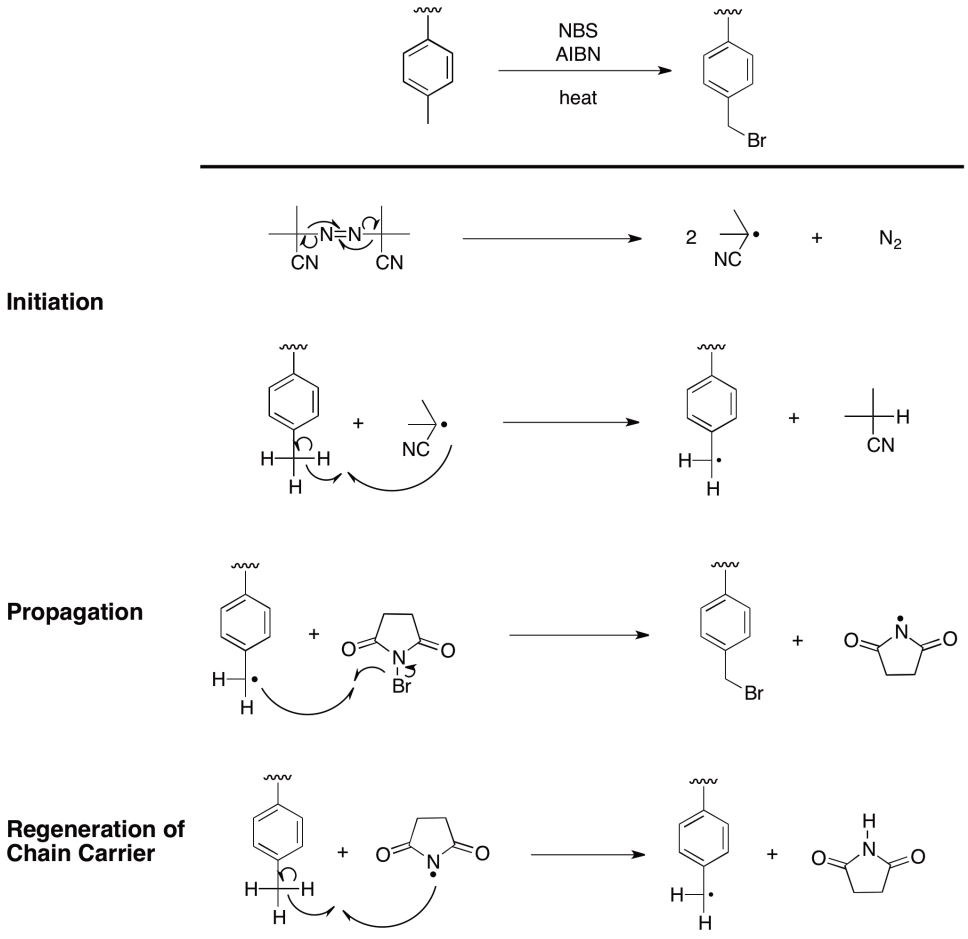

Scheme 10. Free Radical Bromination Mechanism.

First, initiation occurs in which AIBN free radicals are generated via heat/photolysis and the free radical removes a hydrogen atom from a tolyl group leaving behind a free benzylic radical (resonance stabilized). Next, propagation occurs and the

benzylic free radical reacts with the bromine group from NBS generating both the bromo benzyl group and the succinimide radical chain transfer carrier. Finally, the termination step transpires where the succinimide radical removes the hydrogen from the tolyl group. Other termination steps can occur where free radicals react with each other. Dibromination is avoided/minimized due to the 1:1 tolyl/bromo molar ratio and also by the use of dilute reaction conditions.

^{1}H And ^{13}C NMR spectroscopic analyses were used to determine the structure of polymers **3a-e** and an overlay of the ^{1}H NMR spectra for both polymers **3c** and **3e** is shown in **Figure 15** to display a comparison and help identify certain peaks. The polymer **3c** spectrum displays 15 distinct peaks, where as the **3e** spectrum displays 13 distinct peaks and can be attributed to the lack of the presence of monomer **1b.** Polymers **3c** and **3e** contain the addition of 5 new proton signals **a, b, c, d, e** by comparison with polymers **2c** and **2e** due to the introduction of the bromo group. The bromo group caused a downfield shift of peak **i** because it acts as an electron-withdrawing group. The percent bromination of tolyl groups for both polymers **3c** and **3e** was found to be 60.0% and 57.1%, respectively, by assigning the bisphenol-A methyl groups as the standard, 6H. Protons **a** and **a'** appear as triplets at 6.79 and 6.81 ppm, respectively, and the integration of each peak in both polymers **3c** and **3e** confirmed the extent of bromination as well as the rest of the aromatic proton integration.

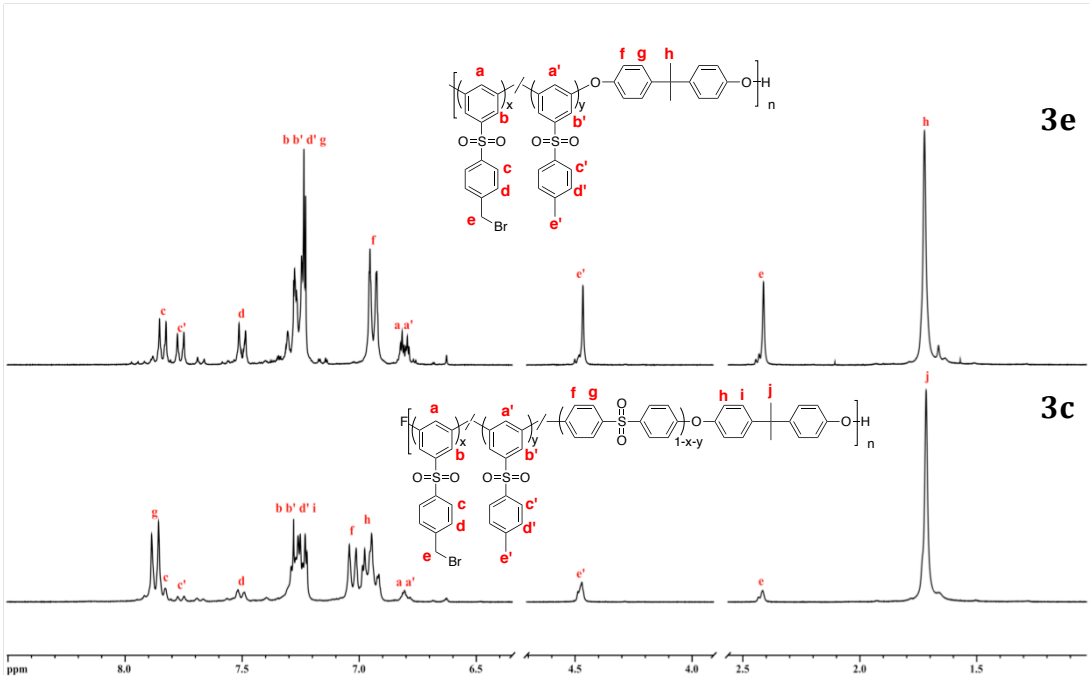

Figure 15. Overlay of 300 MHz ^{1}H NMR spectra ($CDCl_3$) of **3c** and **3e**.

The ^{13}C NMR spectrum of polymer **3c** consists of 35 unique singlet signals and polymer **3e** consists of 27 distinct singlet signals as shown in **Figure 16**. Both polymers **3c** and **3e** contain 9 new signals with the addition of the 3,5-*meta* brominated repeat unit in by comparison with polymers **2a-e**. Proton **e** demonstrates a downfield shift due to the electron withdrawing bromo group and occurs at 31.3 ppm. This signal, as well as the other 8 aromatic carbons (**a, b, c, d**, **f, g, h, i**) confirms a successful radical bromination synthesis. The 9 carbon signals **a'-i'** confirm a certain percentage of non-brominated monomer **1c** is still present. Twelve distinct signals appear in the bisphenol-A aromatic region of polymer **3c** due to the influence in connection of either monomer subunits: **1b,**

1c, or the brominated version of **1c**, whereas only 8 distinct signals occur in the same aromatic region of polymer **3e** because it lacks the presence of monomer subunit **1c**.

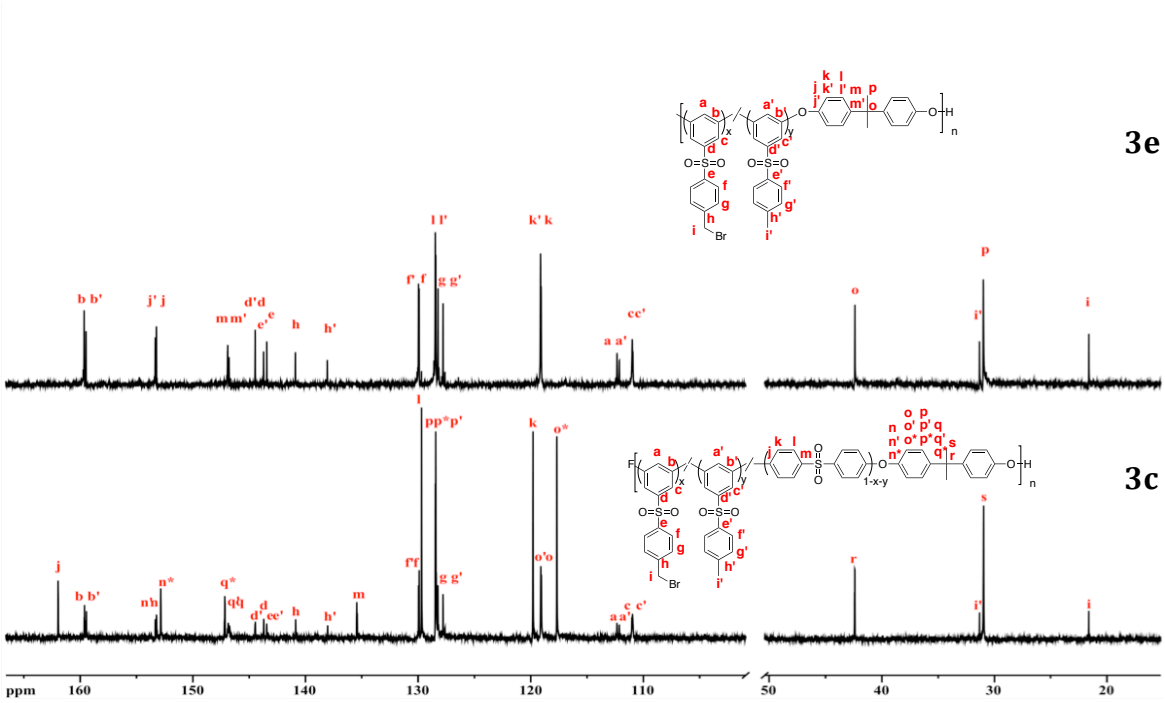

Figure 16. Overlay of 75.5 MHz ^{13}C NMR spectra ($CDCl_3$) of **3c** and **3d**.

In addition to spectroscopic analysis, polymers **3a-e** were characterized for both molecular weight and thermal properties to more accurately detail the progression of the PAES to functionalized cationic PAES for AEMs. The same procedure for the previous polymers **2a-e** was duplicated to obtain the molecular weights of the new polymers **3a-e**. The M_n revealed a range between 22,800-84,500 Daltons with a dispersity range between 3.1-6.0. The SEC trace of polymer **3c** is shown in **Figure 17** and the molecular weights and polymer dispersities are found in **Table 3.**

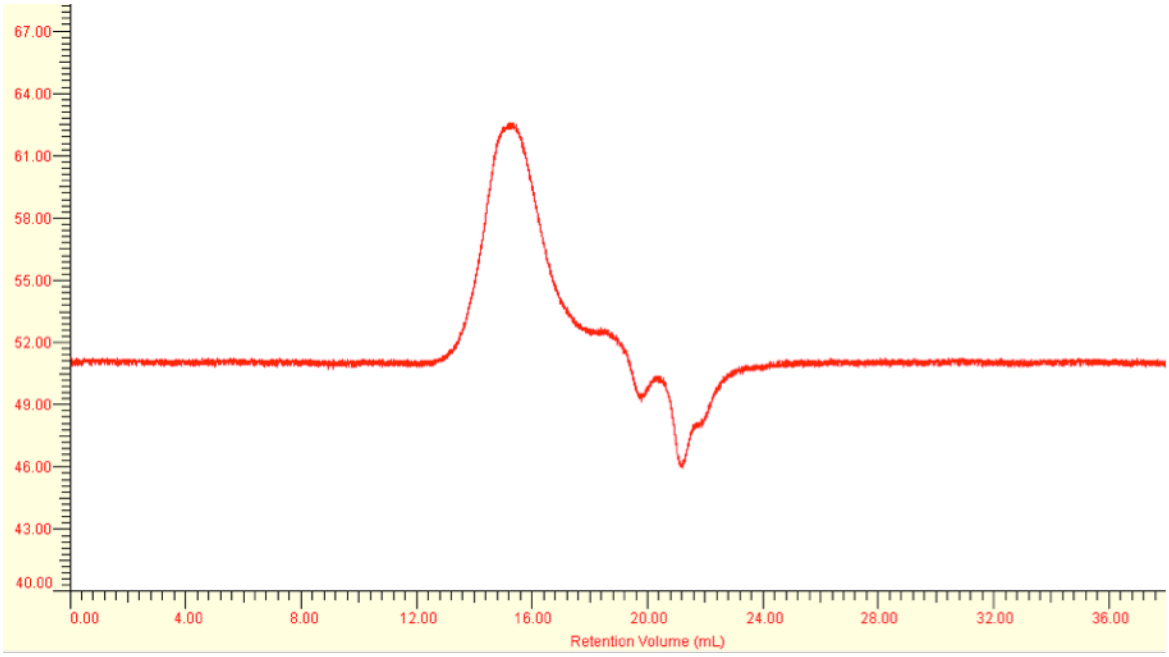

Figure 17. SEC Trace of **3c**.

Table 3. Molecular Weight and Dispersity Values of Polymers **3a-e**.

Polymer	% Bromination	M_n (g/mol)	Đ
3a	39.0	35,200	3.6
3b	58.0	46,500	5.4
3c	60.0	84,500	6.0
3d	64.0	54,500	4.2
3e	57.0	22,800	3.1

The polymers **3a-e** displayed an increase in both M_n and Đ. This rise can be attributed to the addition of the bromo benzyl group; however, the increase appears to be larger than expected and this could possibly attributed to further removal of cyclic

oligomers. Polymers **3a-d** displayed high enough molecular weights for the casting of practical flexible films, but polymer **3e** was of insufficient molecular weight, or the backbone was too rigid, to allow for chain entanglements and ultimately led to a brittle film.

TGA and DSC were used to determine the thermal properties of polymers **3a-e.** The same method was used from the previous polymers **2a-e** to determine both the onset degradation temperatures and the glass transition temperatures. The TGA and DSC traces are shown in **Figure 18** and **Figure 19** as overlays.

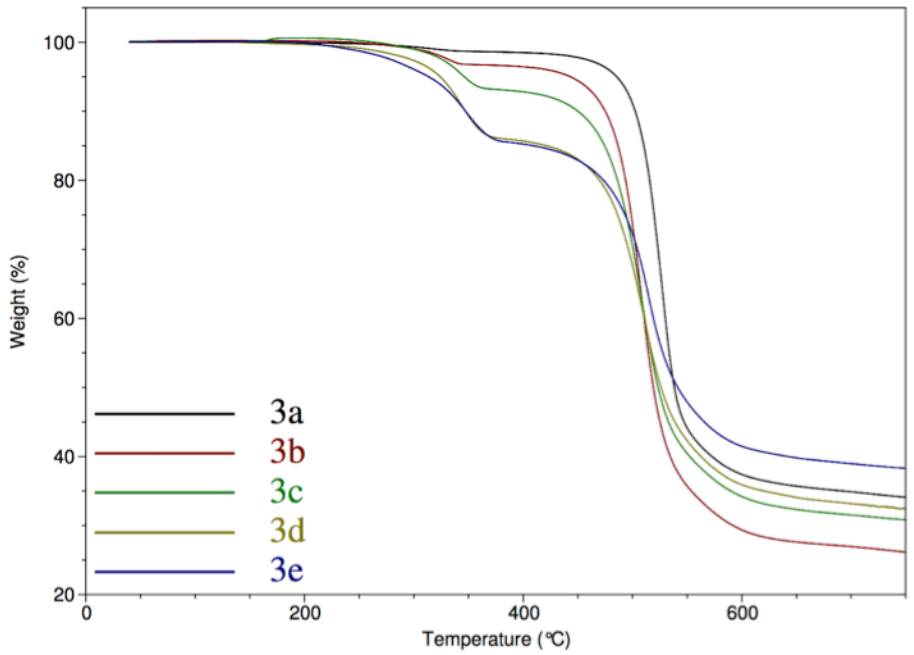

Figure 18. TGA Traces of Polymers **3a-e**.

The TGA thermograms for all polymers **3a-e** show that there are two degradation steps. The first degradation step corresponds to the loss of the bromo benzyl group. This observation is based on the theoretical calculated percentage weight loss versus the experimental percentage weight loss for all polymers **3a-e** and the first step identity was confirmed by this process as the bromo benzyl group. All of the polymers **3a-e** exhibit moderate thermal stability with $T_{d\text{-}onset}$ values above 250 °C as shown in **Table 4**.

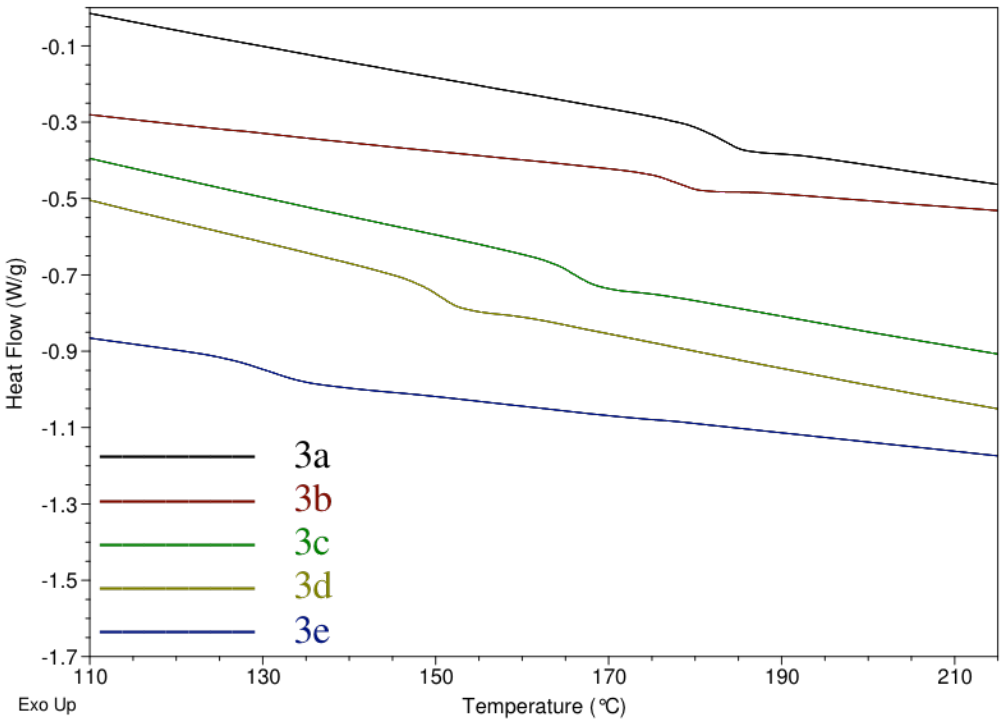

Figure 19. DSC Traces of Polymers **3a-e**.

Table 4. Thermal data for Polymers **3a-e**.

Polymer	$T_{d\text{-}1st\text{-}step}$ (°C)	$T_{d\text{-}2nd\text{-}step}$ (°C)	T_g (°C)
3a ($x_{3.9}$-$y_{6.1}$)	257	486	183
3b ($x_{14.5}$-$y_{10.5}$)	264	443	178
3c (x_{30}-y_{20})	261	346	166
3d ($x_{57.6}$-$y_{32.4}$)	274	324	156
3e (x_{57}-y_{43})	260	314	131

*x and y refer to the % of aminated/tolyl groups compared to bisphenol-A and monomer (**1b**) = 1-x-y

3.5. Amination of Brominated PAES with Methylimidazole (4a-e)

A series of brominated poly(aryl ether sulfone)s were functionalized by the amination of the pendent bromo benzyl sulfonyl groups with 1-methylimidazole via a substitution reaction (Menshutkin) shown in **Scheme 11**. Polymers **3a-e** were first dissolved in distilled DMF and then 1-methylimidazole was added at a 10 (1-MI) to 1 (bromo benzyl) molar ratio to the systems. All reactions were heated to 80 °C for 48 h, after which the polymers were precipitated into ethyl acetate and then stirred in acetone to remove any excess 1-methylimidazole. The polymers were dried at 80 °C for 48 h under vacuum or until a constant mass was achieved.

^{1}H and ^{13}C NMR spectroscopic analyses were used to determine the structures of polymers **4a-e** and the ^{1}H NMR spectrum for polymer **4b** is shown in **Figure 20**. The polymer **4b** spectrum displays 19 distinct hydrogen peaks as well as 8 solvent hydrogen peaks

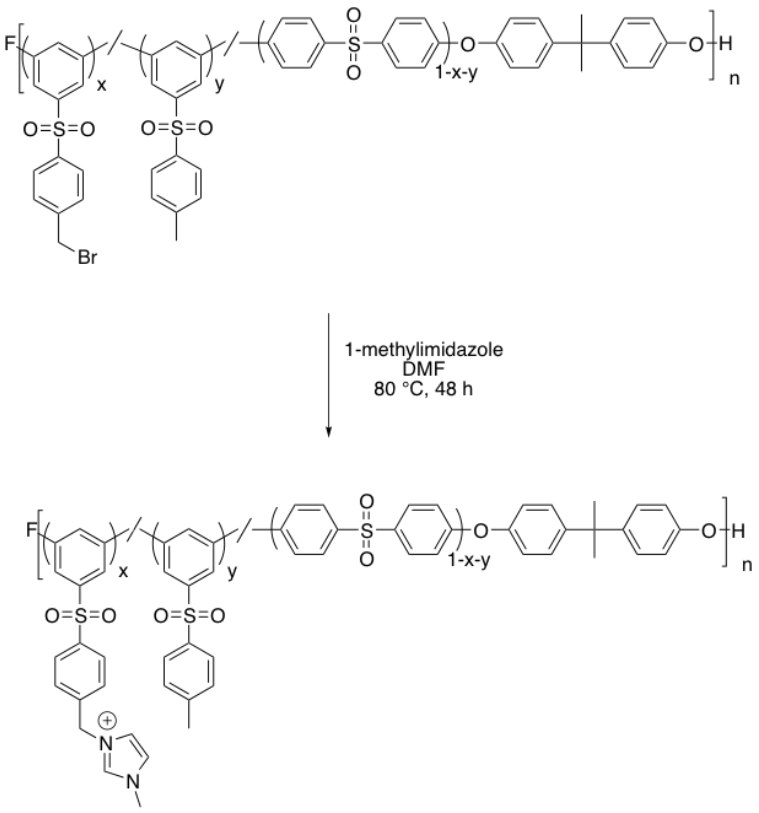

Scheme 11. Synthesis of Polymers **4a-e** via Amination with 1-methylimidazole

The presence of the solvent peaks can be attributed to the difficulty of removal due to the cationic 1-methylimidazole groups and also not drying the polymer above 80 °C to prevent degradation. Protons **e** and **k** are singlets and occur at 5.54 (0.3H) and 9.24 ppm (0.2H), respectively. Both these proton peaks and integration values demonstrate complete substitution of the bromo benzyl groups by 1-methylimidazole for polymer **4b** and also polymers **4a**, **4c**, **4d**, and **4e**. Also the lack of the bromo benzyl hydrogen peak at 4.60 ppm confirms this assertion.

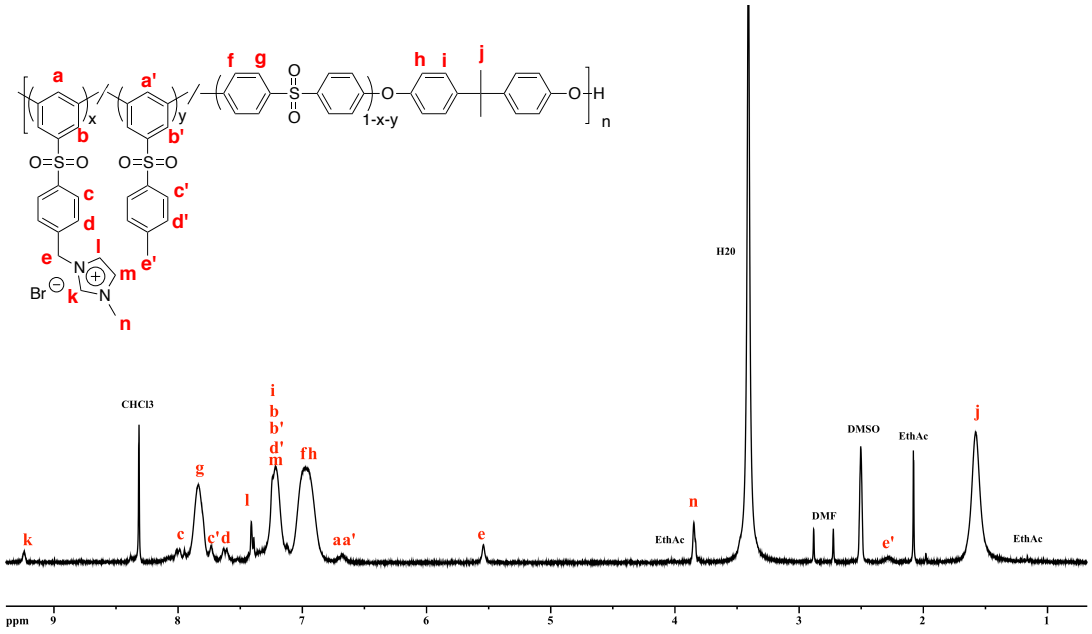

Figure 20. 300 MHz ^{1}H NMR spectrum (DMSO-d_6) of **4b**.

The ^{13}C NMR spectrum of polymer **4b** consists of 36 unique singlet signals and 5 solvent peaks as shown in **Figure 21**. The 1-methylimidazole substitution of the bromo benzyl group causes a downfield shift of carbon atom **i** from 31.6 to 51.5 ppm, and also the addition of carbon atom signals **t**, **u**, **v**, and **e** occurring at 36.9, 122.9, 124.6, and 137.5 ppm, respectively. The bisphenol-A sub-unit produced 12 distinct carbon signals due to being able to distinguish between the 4,4'-*para* subunit and both of the 3,5-*meta* subunit monomers.

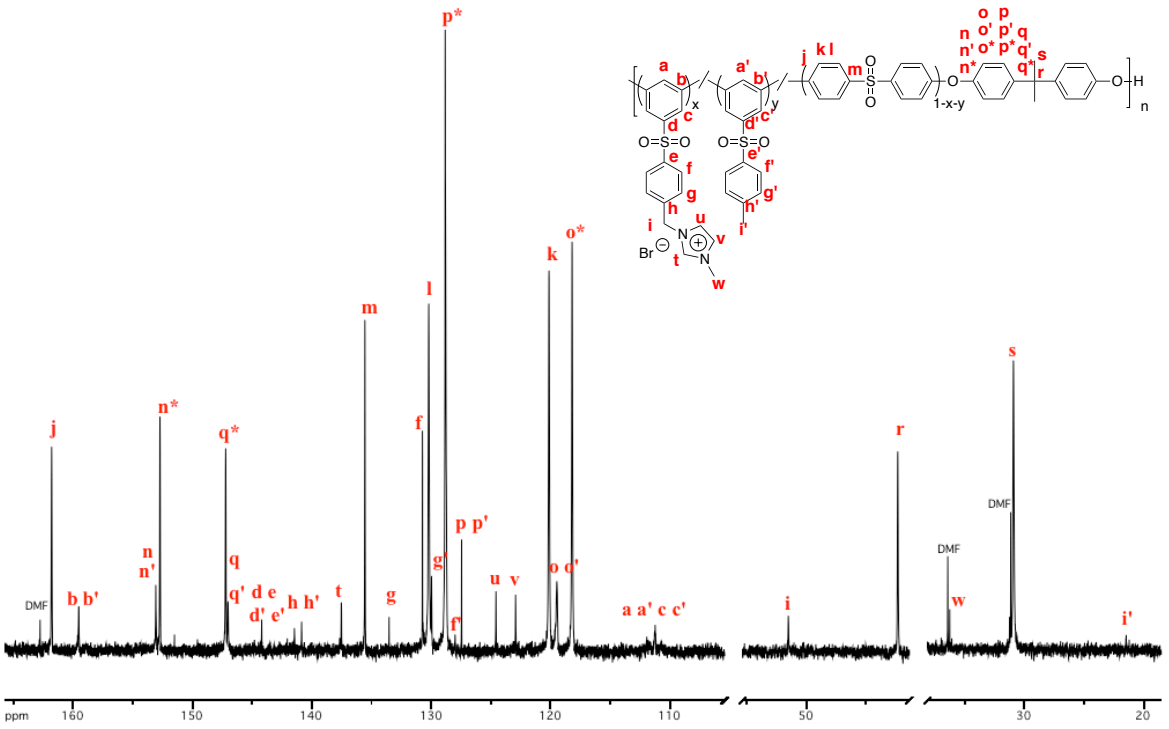

Figure 21. 75.5 MHz ^{13}C NMR spectrum (DMSO-d_6) of **4b**.

In addition to spectroscopic analysis, polymers **4a-e** were characterized for both thermal and anionic exchange membrane properties (AEM properties will be discussed in a later section. Polymers **4a-e** were cast as films from DMF and dried at 80 °C for 48 h or until a constant mass was reached. TGA and DSC were used to determine the thermal properties of **4a-e** membranes and the same method was used as for the previous polymers to determine both the onset degradation temperatures and the glass transition temperatures; however, the DSC analysis failed to determine the T_g due to apparent functional group deterioration. The TGA traces of **4a-e** are shown in **Figure 22**.

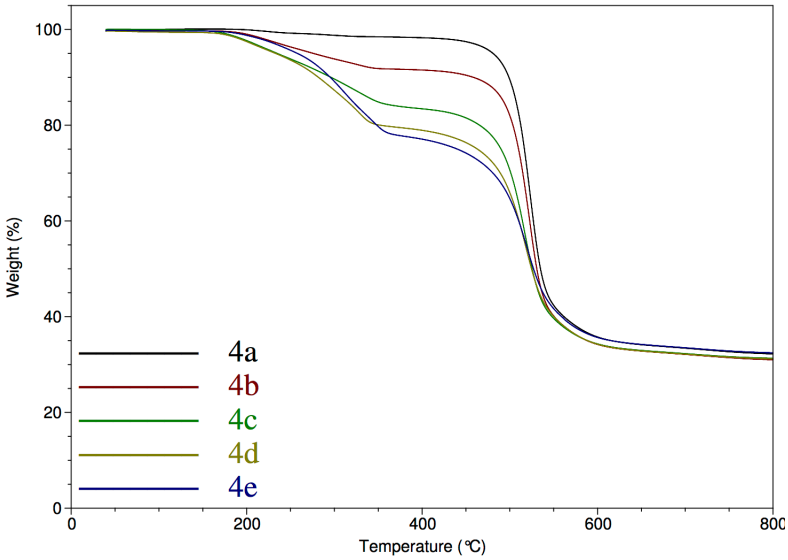

Figure 22. TGA Traces of Polymers **4a-e**.

The TGA thermograms for all polymers **4a-e** show that there are two degradation steps with the first step loss corresponding to the 1-methylimidazole cationic groups and the second step loss being attributable to the polymer backbone. All of the polymers **4a-e** exhibit moderate thermal stability with $T_{1st\text{-}onset}$ values above 180 °C as shown in **Table 5**.

Table 5. Thermal data for Polymers **4a-e**.

Polymer	4a ($x_{3.9}$-$y_{6.1}$)	4b ($x_{14.5}$-$y_{10.5}$)	4c (x_{30}-y_{20})	4d ($x_{57.6}$-$y_{32.4}$)	4e (x_{57}-y_{43})
$T_{1st\text{-}step}$ (°C)	**184**	**186**	**192**	**183**	**180**
$T_{2nd\text{-}step}$ (°C)	**500**	**498**	**493**	**484**	**483**

*x and y refer to the % of aminated/tolyl groups compared to bisphenol-A and monomer (**1b**) = 1-x-y

3.6. Amination of Brominated PAES with Trimethylamine (5a-e)

A series of brominated poly(aryl ether sulfone)s was functionalized by the amination of the pendent bromo benzyl groups with trimethylamine via a substitution reaction (Menshutkin) by two different methods which are shown in **Scheme 12**. In the first method, polymers **3a, 3b, and 3e** were dissolved in distilled DMF and then trimethylamine was added at a 10 (TMA) to 1 (bromo benzyl) molar ratio to the systems. All reactions were conducted at rt for 48 h, after which the polymers were precipitated into ethyl acetate and then stirred in acetone to remove any starting materials. The polymers were dried at 80 °C for 48 h under vacuum or until a constant mass was achieved.

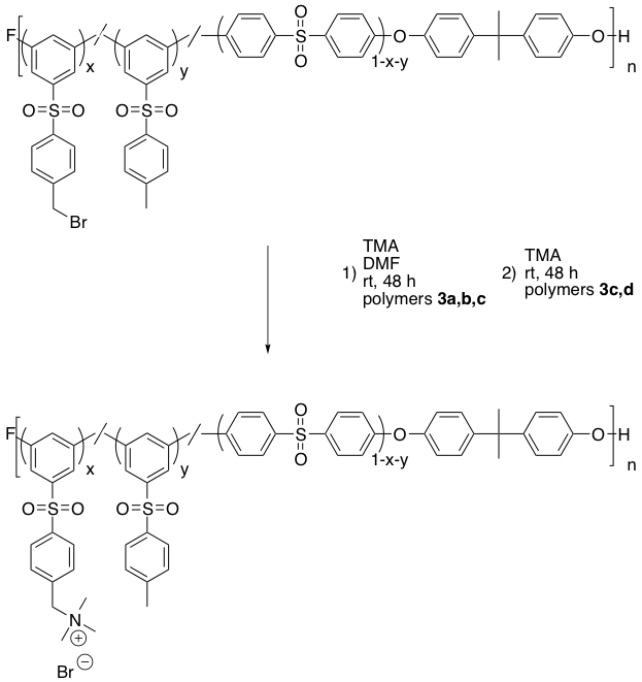

Scheme 12. Synthesis of Polymers **5a-e** via Amination with Trimethylamine

Polymers **5c** and **5d** had solubility issues using this method and so an alternative method was performed in which brominated polymers were first cast into films and then submerged into stirring 45% trimethylamine, at rt, for 48 h. The films were then washed with DI water to remove any starting materials and dried under vacuum at 80 °C for 48 h or until a constant mass was reached.

^{1}H and ^{13}C NMR spectroscopic analyses were used to determine the structure of polymers **5a, 5b,** and **5e**; the ^{1}H NMR spectrum for polymer **5e** is shown in **Figure 23**.

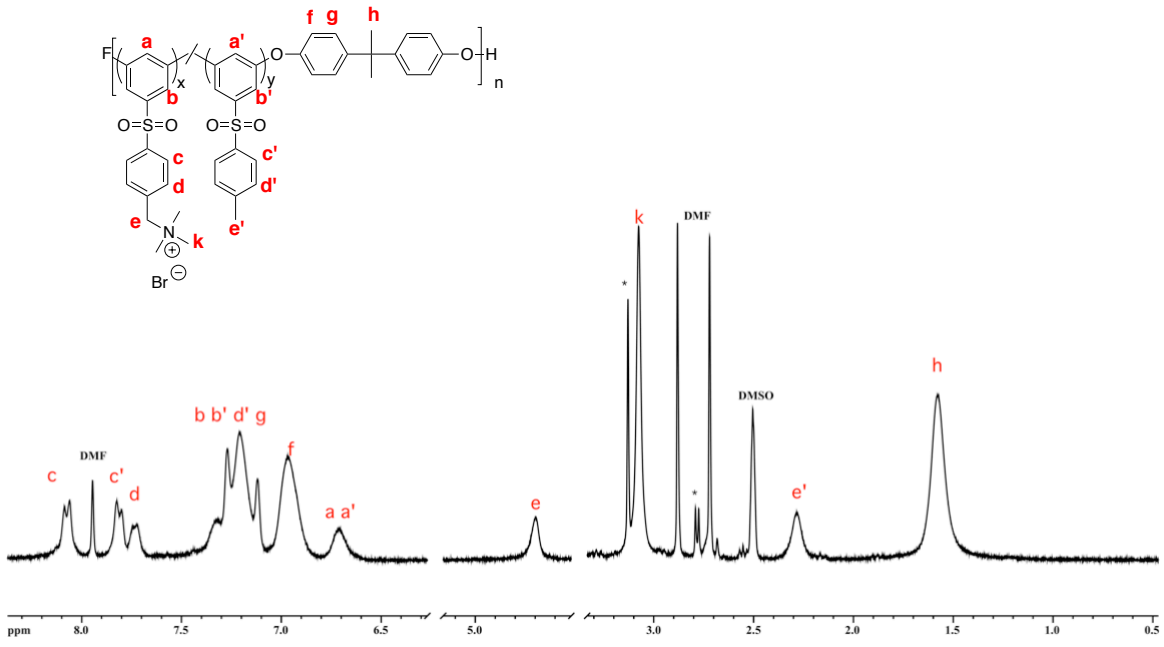

Figure 23. 300 MHz ^{1}H NMR spectrum (DMSO-d_6) of **4e**.

The polymer **5a** spectrum displays 14 distinct polymer peaks as well as 5 solvent peaks. The presence of the solvent peaks can be attributed to the difficulty of removal due to the cationic quaternary groups and also not drying the polymer above 80 °C to prevent degradation. Protons **e** and **k** are singlets and occur at 4.70 (1.0H), and 3.08 (5.3H), respectively. Both these proton peaks demonstrate complete substitution of the bromo benzyl groups by trimethylamine for polymer **4e**. Also the lack of the bromo benzyl hydrogen peak at 4.60 ppm confirms this assertion.

The ^{13}C NMR spectrum of polymer **5e** consists of 29 unique singlet signals and 6 solvent peaks as shown in **Figure 24**.

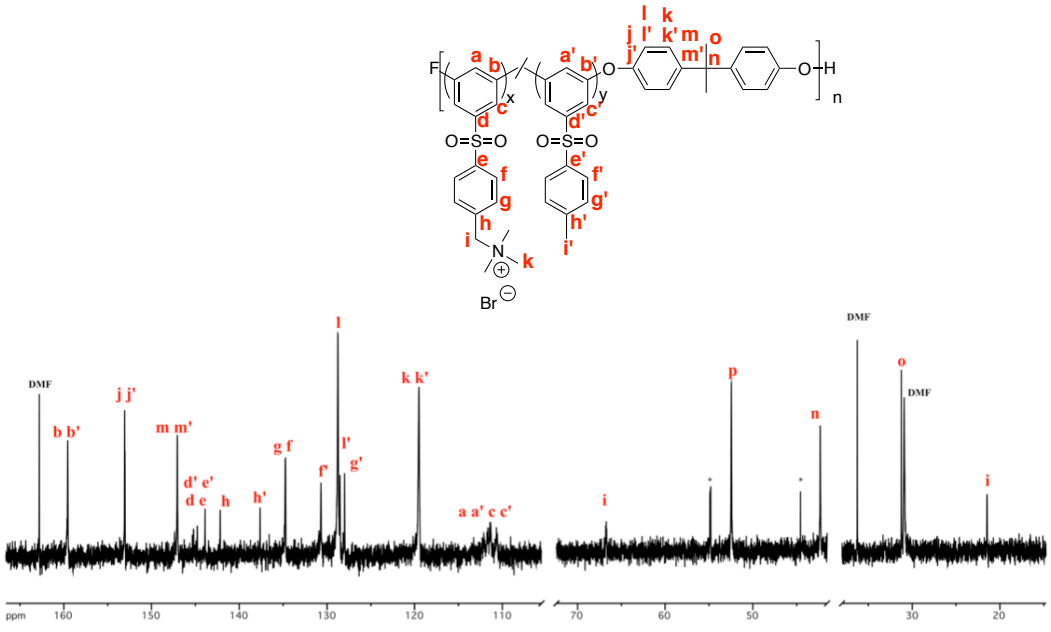

Figure 24. 75.5 MHz ^{13}C NMR spectrum (DMSO-d_6) of **5e**.

The trimethylamine substitution of the bromo benzyl group causes a down field shift of carbon atom **i** from 31.6 to 66.7 ppm, and this shift and the lack of the bromo benzyl peak at 31.6 ppm confirms complete amination of the bromo benzyl groups. The addition of the carbon atom signal **p** occurring at 52.5 ppm results from the cationic quaternary methyl groups. The bisphenol-A sub-unit produced 8 distinct carbon signals (**j**, **j'**, **k**, **k'**, **l**, **l'**, **m**, **m'**) due to being able to distinguish between the aminated and tolyl version of the 3,5-*meta* subunit monomers.

Polymers **5c** and **5d** were analyzed using FT-IR spectroscopic analysis to investigate and confirm the amination of the bromo benzyl groups by trimethylamine. The FT-IR spectrum for polymer **5c** is shown in **Figure 25** (A) with air as the background. The FT-IR **5c** polymer spectrum (A) contains stretching regions at: 1500 cm^{-1} (C-C aromatic stretching), 2960 cm^{-1} (C-H alkyl stretching), 3050 cm^{-1} (C-H aromatic stretching), and 3200-3700 cm^{-1} (O-H stretching), respectively

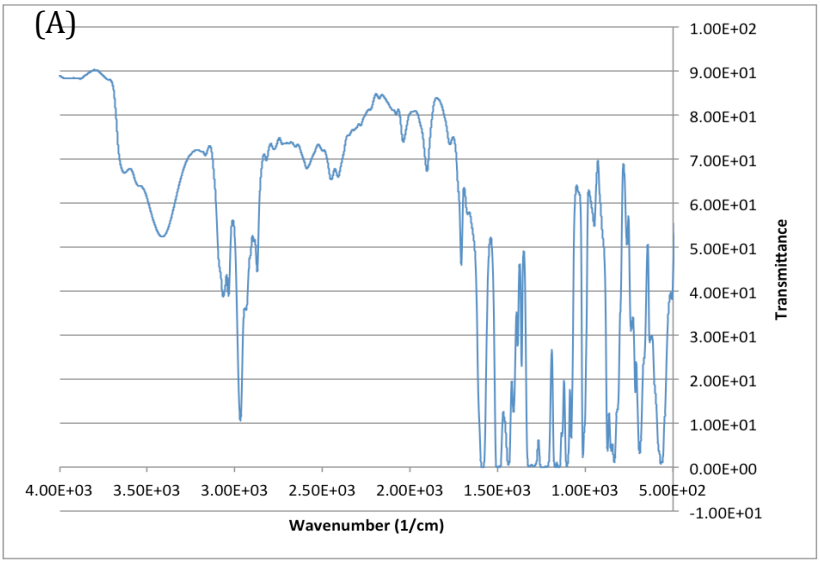

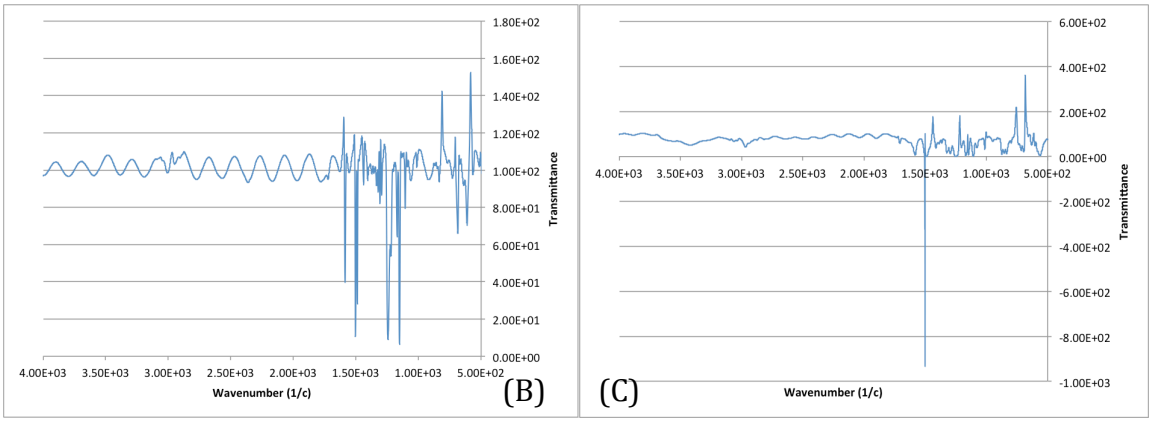

Figure 25. FT-IR Spectra: Polymer **5c** (A) with air background, Polymer **3c** (B) with **2c** background, Polymer **5c** (C) with **2c** background

It was difficult to determine the displacement of the bromo benzyl group due to a large broad signal occurring in the 1150-1250 cm^{-1} region (possibly due to the film being too thick). Thus, a different approach was taken where polymer **2c** was used as the background for both polymers **3c** and **5c** and the spectra are shown in **Figure 25** (B & C). The FT-IR spectrum for polymer **3c** (B) exhibits a bromo benzyl peak at 1225 cm^{-1} (C-Br stretching) and the FT-IR spectrum for polymer **5c** (B) indicated the substitution of the bromo benzyl group due to the lack of the 1225 cm^{-1} peak by trimethylamine.

In addition to spectroscopic analyses, polymers **5a-e** were characterized for both thermal and anionic exchange membrane properties (AEM properties will be discussed in a later section).

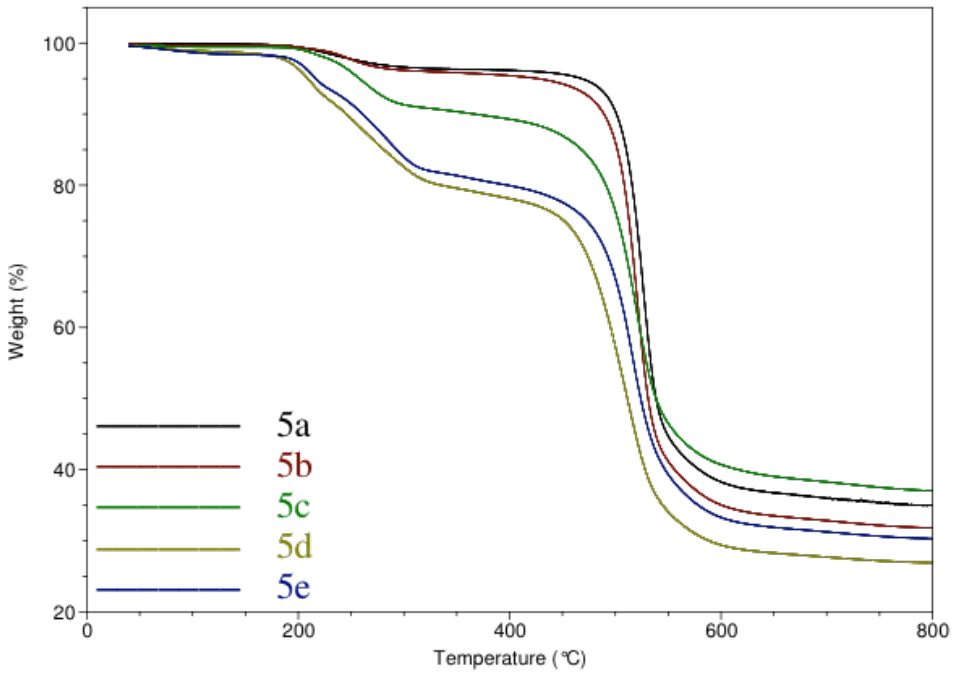

Figure 26. TGA Traces of Polymers **5a-e**.

Polymers **5a**, **5b**, and **5e** were cast as films from DMF and dried at 80 °C for 48 h or until a constant mass was reached. TGA and DSC were used to determine the thermal properties of **5a-e** membranes and the same method was used as for the previous polymers to determine both the onset degradation temperatures and the glass transition temperatures; however, once again the DSC analysis failed to determine the T_g due to functional group deterioration. The TGA traces of **5a-e** are shown in **Figure 26.**

The TGA thermograms for all polymers **5a-e** show that there are two degradation steps with the first step loss corresponding to the trimethylamine cationic groups and the

second step loss being attributable to the polymer backbone. All of the polymers **5a-e** exhibit moderate thermal stability with $T_{1st\text{-}onset}$ values above 189 °C as shown in **Table 6.** It is worth noting that molecular weight and dispersity were not obtainable due to insolubility with the SEC eluent, THF/ 5% (v/v) acetic acid solution.

Table 6. Thermal data for Polymers **5a-e**.

Polymer	5a ($x_{3.9}$-$y_{6.1}$)	5b ($x_{14.5}$-$y_{10.5}$)	5c (x_{30}-y_{20})	5d ($x_{57.6}$-$y_{32.4}$)	5e (x_{57}-y_{43})
$T_{1st\text{-}step}$ (°C)	**196**	**202**	**204**	**189**	**191**
$T_{2nd\text{-}step}$ (°C)	**499**	**493**	**489**	**476**	**484**

*x and y refer to the % of aminated/tolyl groups compared to bisphenol-A and monomer (**1b**) = 1-x-y

3.7. Amination of Brominated PAES with *N,N*-dimethylhexadecylamine (6a-e)

A series of brominated poly(aryl ether sulfone)s were functionalized by the amination of the pendent bromo benzyl groups with *N,N*-dimethylhexadecylamine via a substitution reaction (Menshutkin) as shown in **Scheme 13**. Polymers **3a-e** were dissolved in distilled DMF and then *N,N*-dimethylhexadecylamine was added at a 10 (DMHDA) to 1 (bromo benzyl) molar ratio to the systems. All reactions were conducted at 80 °C for 48 h, after which polymers **6a** and **6b** were precipitated into ethyl acetate and then stirred in acetone to remove any starting materials. Polymers **6c, 6d,** and **6e** were cast on to a glass plate after the completed reaction and submerged in acetone to remove any starting

materials. The polymers were dried at 80 °C for 48 h under vacuum or until a constant mass was achieved.

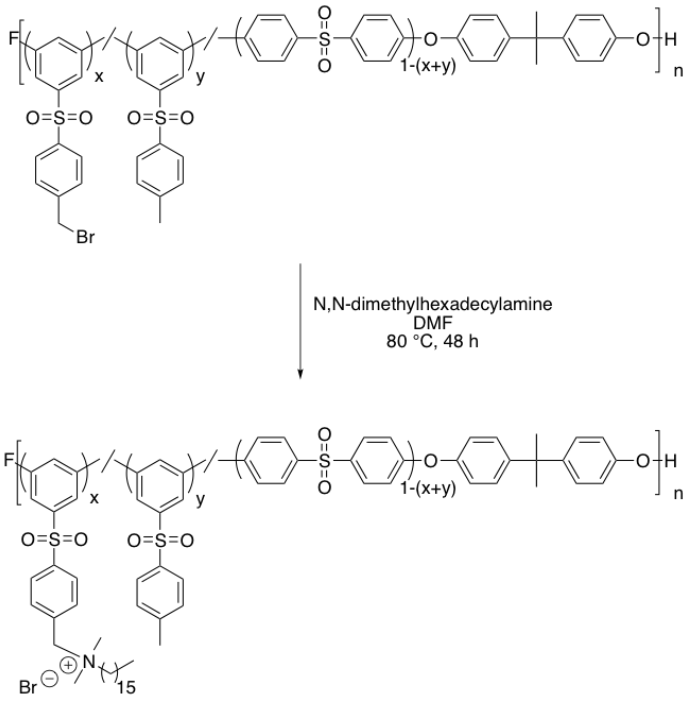

Scheme 13. Synthesis of Polymers **6a-e** via Amination with *N,N*-dimethylhexadecylamine

^{1}H and ^{13}C NMR spectroscopic analyses were used to determine the structure of polymers **6a-b** and the ^{1}H NMR spectrum for polymer **6b** is shown in **Figure 27**. The polymer **6b** spectrum displays 20 distinct hydrogen peaks as well as 9 solvent hydrogen peaks. The presence of the solvent peaks can be attributed to the difficulty of removal due to the cationic quaternary groups and also not drying the polymer above 80 °C to prevent

degradation. Proton **e** is a singlet and occurs at 4.62 (0.2H integration) and the lack of the bromo benzyl peak confirms the complete substitution by *N,N*-dimethylhexadecylamine for polymer **4e**. Protons **k**, **l**, **m**, **n**, and **o** were identified as those from the cationic quaternary amine groups.

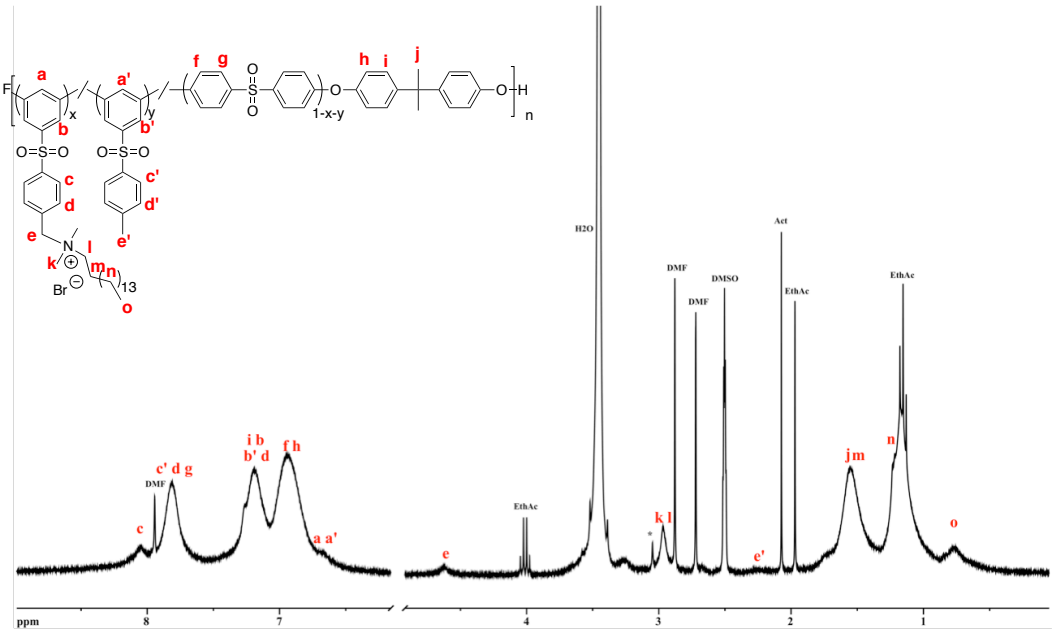

Figure 27. 300 MHz ^{1}H NMR spectrum (DMSO-d_6) of **6b**.

The ^{13}C NMR spectrum of polymer **6b** consists of 42 unique singlet signals and 7 solvent peaks as shown in **Figure 28**. The DMHDA substitution of the bromo benzyl group causes a downfield shift of carbon atom **i** from 31.6 to 64.5 ppm and the lack of the bromo benzyl peak at 31.6 ppm confirms complete amination of the bromo benzyl groups. The addition of the carbon atom signal **t** occurring at 49.8 ppm results from the cationic quaternary methyl groups. Carbon atom **u** signal was lost in the DMSO solvent peak and

could not be accurately observed. The aliphatic carbon atom peaks: **v**, **w**, **x**, **y**, and **z** are found at 31.7, 29.5, 26.3, 22.5, and 14.3 ppm, respectively.

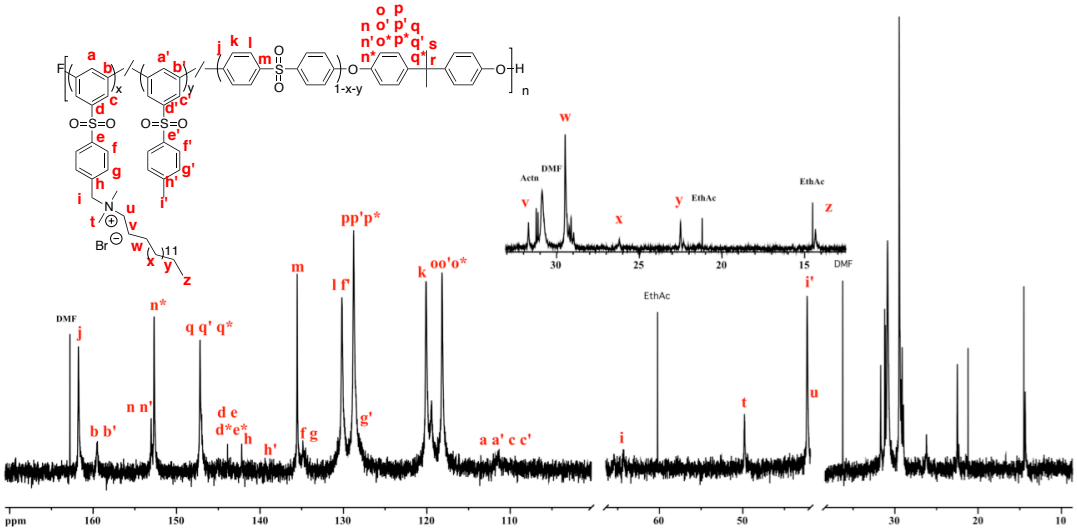

Figure 28. 75.5 MHz ^{1}H NMR spectrum (DMSO-d_6) of **6b**.

Polymers **6c-e** were analyzed using FT-IR spectroscopy to investigate and confirm the amination of the bromo benzyl groups by *N,N*-dimethylhexadecylamine. The FT-IR spectrum for polymer **6d** is shown in **Figure 28** (A) with air as the background. The FT-IR **6d** polymer spectrum (A) contains stretching regions at 1500 cm^{-1} (C-C aromatic stretching), 2960 cm^{-1} (C-H alkyl stretching), 3050 cm^{-1} (C-H aromatic stretching, and 3200-3700 cm^{-1} (-O-H stretching), respectively.

It was difficult to determine the displacement of the bromine from the bromo benzyl group due to a large broad signal occurring in the 1150-1250 cm^{-1} region. Thus, a different approach was taken where polymer **2d** was used as the background for polymer

6d and the spectrum is shown in **Figure 28** (B). The FT-IR **6d** polymer spectrum (B) confirms the substitution of the bromine from the bromo benzyl group by trimethylamine due to the lack of the 1225 cm^{-1} peak.

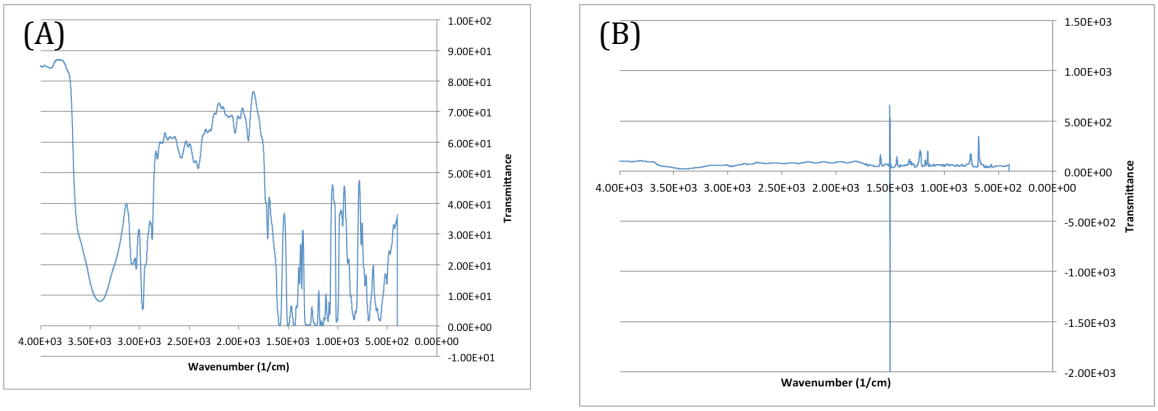

Figure 29. FT-IR Spectra: Polymer **6d** (A) with air background, and Polymer **5c** (B) with **2c** background.

In addition to spectroscopic analyses, polymers **6a-e** were characterized for both thermal and anionic exchange membrane properties (AEM properties will be discussed in later section). Polymers **6a** and **6b** were cast as films from DMF and dried at 80 °C for 48 h or until a constant mass was reached. TGA and DSC were used to determine the thermal properties of **6a-e** membranes and the same method was used as for the previous polymers to determine both the onset degradation temperatures and the glass transition temperatures; however, once again the DSC analysis failed to determine the T_g due to functional group deterioration. The TGA traces of **6a-e** are shown in **Figure 30.** The

TGA thermograms for all polymers **6a-e** show that there are two degradation steps with the first step loss corresponding to the *N,N*-dimethylhexadecylamine cationic groups and the second step loss being attributable to the polymer backbone. All of the polymers **6a-e** exhibit moderate thermal stability with $T_{1st\text{-}onset}$ values above 175 °C as shown in **Table 7.** It is worth noting that molecular weight and dispersity were not obtainable due to insolubility in the SEC eluent, THF/ 5% (v/v) acetic acid solution.

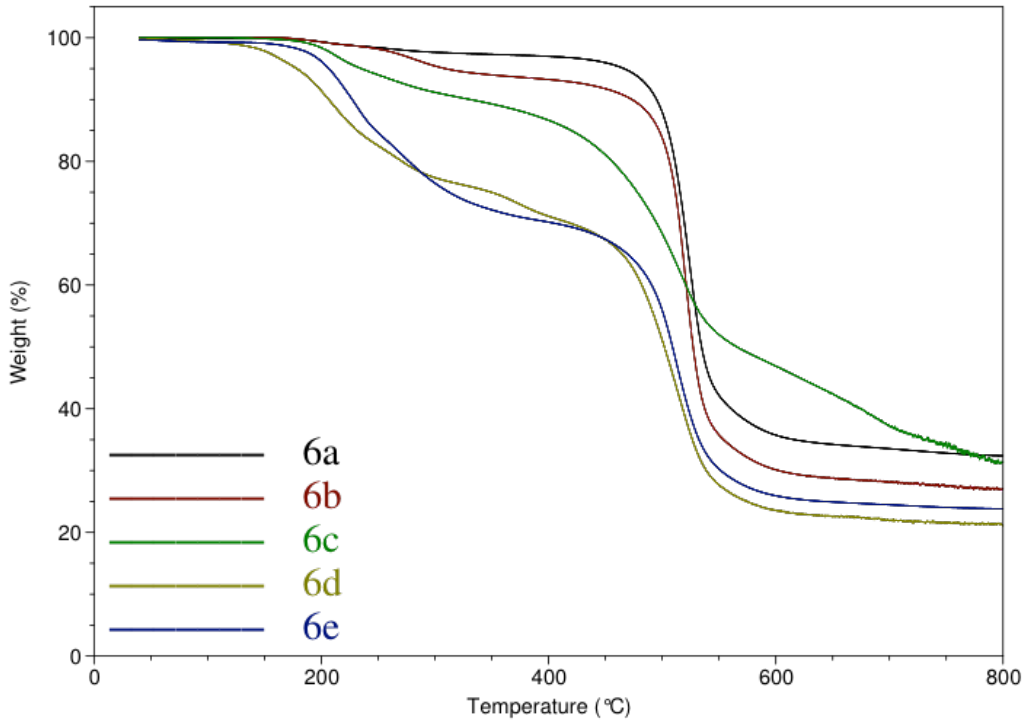

Figure 30. TGA Traces for Polymers **6a-e**.

Table 7. Thermal data for Polymers **6a-e**.

Polymer	6a ($x_{3.9}$-$y_{6.1}$)	6b ($x_{14.5}$-$y_{10.5}$)	6c (x_{30}-y_{20})	6d ($x_{57.6}$-$y_{32.4}$)	6e (x_{57}-y_{43})
$T_{1st\text{-}step}$ (C)	**176**	**179**	**190**	**175**	**176**
$T_{2nd\text{-}step}$ (C)	**499**	**488**	**489**	**475**	**476**

*x and y refer to the % of aminated/tolyl groups compared to bisphenol-A and monomer (**1b**) = 1-x-y

3.8. Anionic Exchange Membrane Characterization

All of the polymers were characterized for typical AEM characteristics, which included both water uptake and ion exchange capacities. Polymer **5e** was the only exception because the membrane proved to be too brittle and broke apart after casting. Water uptake values were determined by first soaking the membranes in 1M NaOH solution in order to exchange the bromine ions with hydroxide ions. The membranes were then washed with DI H_2O and dried at 80 °C under vacuum until a constant mass was reached. The membranes were then placed in DI H_2O for 24 h and then their mass was obtained after blotting excess water off the films. The water uptakes are shown in **Table 8**. Water uptakes values were low and increase as the number of quaternary cationic groups increase, which is expected.

Ion exchange values were attempted by soaking the AEM exchange membranes in a 0.01M HCl solution (20 ml) for 24 h and then back-titrating with 0.01M NaOH solution while monitoring the pH. The titrated endpoints were found by taking the largest maxima in the d(pH) vs dV titration plots. However, the results proved to be too inaccurate and produced some negative IECs and the results are not present in **Table 8**. Thus, a different method is needed to improve upon both accuracy and precision for acquiring the titrated ion exchange capacities. The calculated IEC values of both the bromine and hydroxide forms for all polymers, except **5e,** are shown in **Table 8**. These calculated values were obtained by using **equation 3**. The calculated IEC values increase as the number of quaternary cationic groups is increased, which is expected.

Table 8. Water Uptake % and IEC Values for AEMs.

Polymer	Water Uptake %	$IEC_{calc.}$ (meq/g)
4a ($x_{3.9}$-$y_{6.1}$)	1.8	0.087
4b ($x_{14.5}$-$y_{10.5}$)	2.4	0.314
4c (x_{30}-y_{20})	4.2	0.626
4d ($x_{57.6}$-$y_{32.4}$)	6.4	1.127
4e (x_{57}-y_{43})	7.1	1.114
5a ($x_{3.9}$-$y_{6.1}$)	1.6	0.087
5b ($x_{14.5}$-$y_{10.5}$)	2.2	0.316
5c (x_{30}-y_{20})	4.0	0.635
5d ($x_{57.6}$-$y_{32.4}$)	7.9	1.157
5e (x_{57}-y_{43}) no film	N/A	1.143
6a ($x_{3.9}$-$y_{6.1}$)	1.7	0.086
6b ($x_{14.5}$-$y_{10.5}$)	2.2	0.297
6c (x_{30}-y_{20})	5.2	0.561
6d ($x_{57.6}$-$y_{32.4}$)	13.5	0.931
6e (x_{57}-y_{43})	12.0	0.922

4. Conclusions

A series of poly(aryl ether sulfone)s containing different percentages of 3,5-difluoro-4'-methyldiphenylsulfone and 4,4'-difluorophenylsulfone were synthesized with bisphenol-A by a nucleophilic aromatic substitution. The PAES **2a-e** displayed molecular weights (M_n) in the range between 7000-34,600 g/mol. These polymers exhibited high thermal stabilities with 5% degradation temperatures in excess of 420 °C and showed moderately high glass transitions, all above 134 °C.

The PAES tolyl groups were brominated through a free radical synthesis procedure. The brominated PAES **3a-e** displayed number average molecular weights (M_n) in the range between 22,800-84,500 g/mol. These polymers exhibited moderate thermal stabilities with 1st step loss degradation temperatures in excess of 250 °C and showed moderately high glass transitions, all above 131 °C.

The brominated PAES **3a-e** were successfully functionalized through an amination substitution route with 1-methylimidazole, trimethylamine, and *N,N*-dimethylhexacdecylamine to produce polymers **4a-e**, **5a-e**, and **6a-e**. The NMR spectra and FT-IR spectra confirmed complete amination of the bromo benzyl groups. The films had thermal stabilities in excess of 175 °C.

All of the quaternary cationic polymers were cast into films with the exception of polymer **5e** and analyzed for typical AEM characteristics. Polymers **4a-e** displayed water uptake percentages in the range of 1.8-7.1% and calculated IEC values between 0.087-

1.114 meq/g. Polymers **5a-e** displayed water uptake percentages in the range of 1.6-7.9% and calculated IEC values between 0.087-1.157 meq/g. Polymers **6a-e** displayed water uptake percentages in the range of 1.8-13.5% and calculated IEC values between 0.086-0.922 meq/g.

Titrated ion exchange capacities were not obtained due to the crude titration method that was used and need to be acquired by a different technique such as the use of an automatic titrator.

Overall, a series of poly(aryl ether sulfone)s with varying percentages of ammonium groups, located on truly pendent positions, was prepared and characterized for potential use as anionic exchange membranes for AAEMFCs.

5. Future Work

These anionic exchange membranes need to be more thoroughly investigated for both titrated ion exchange capacities and hydroxide conductivity for their potential use as anionic exchange membranes. It would also be wise, to improve upon the AEM stability by adding an oxybenzene ring spacer that further moves the cationic group away from the backbone and prevents deterioration of the PAES backbone by hydroxide ions through increased microphase separation between the polymer backbone and cationic side groups.

6. References

1. United State Energy Information Administration **Today In Energy**. *https://www.eia.gov/todayinenergy/detail.cfm?id=12251#* (accessed April, 2016).

2. Shafiee, Shahriar; Topal, Erken. When will fossil fuels be diminished? *Energy Policy* **2009**, 37, 181-189.

3. Manahan, S. E. *Environmental Science and Technology: a Sustainable Approach to Green Science and Technology*; CRC/Tayor & Francis: Boca Raton, 2007.

4. United State Department of Energy Energy **Department Invests $10M Through the Fuel Cell Technologies Incubator Funding Opportunity to Support Innovations in Fuel Cell and Hydrogen Fuel Technologies.** *http://energy.gov/eere/fuelcells/articles/energy-department-invests-10m-through-fuel-cell-technologies-incubator* (accessed April 20, 2016).

5. Behling, N. H. *Fuel Cells: Current Technology Challenges and Future Research Needs*; Elsevier: Amsterdam, **2013**;, pp 1-3.

6. Pu, Hongting. *Polymers for PEM Fuel Cells;* John Wiley & Sons: Hoboken, New Jersey, **2014**.

7. Goswami, D. Y.; Kreith, F. *Energy Efficiency And Renewable Energy Handbook, Second Edition*; CRC Press: Boca Raton, Floridia, **2016**.

8. Mench, M. M. *Fuel Cell Engines*; John Wiley & Sons: Hoboken, NJ, **2008**.

9. Eikerling, M.; Kulikovsky, A. A. *Polymer Electrolyte Fuel Cells: Physical Principles of Materials and Operation*; CRC Press: Boca Raton , Floridia, **2015**.

10. Hickner, M. A.; Ghassemi, H.; Kim, Y. S.; Einsla, B. R.; McGrath, J. E., *Chem. Rev*. **2004**, 104 (10), 4587-4612.

11. Gierke, T.D.; Munn, G. E.; Wilson, F.C. *J. Polym. Sci. Polym. Phys. Ed.*, **1981,** 19, 1687.

12. Kreuer, K.D.; Paddison, S. J.; Spohr, E.; Schuster, M., Chem. Rev.**2004**, 104 (10), 4637- 4678.

13. Srinivasan, S.; Velev, O. A.; Parthasarathy, A.; Manko, D. J.; Appleby, A. J. *J. Power Sources* **1991**, *36*, 299.

14. United State Department of Energy Energy **Fuel Cell Technologies Office Multi-Year Research, Development, and Demonstration Plan.** http://energy.gov/eere/fuelcells/downloads/fuel-cell-technologies-office-multi-year-research-development-and-22 (accessed March, 2016)

15. Houchins, C.; Kleen, G.; Spendelow, J.; Kopasz, J.; Peterson, D.; Garland, N.; Ho, D.; Marcinkoski, J.; Martin, K.; Tyler, R.; Papageorgopoulos, D. U.S. DOE Progress Towards Developing Low-Cost, High Performance, Durable Polymer Electrolyte Membranes For Fuel Cell Applications. *Membranes*. **2012**, *2*, 855–878.

16. Hickner, M. A.; Ghassemi, H.; Kim, Y. S.; Einsla, B. R.; Mcgrath, J. E. Alternative Polymer Systems For Proton Exchange Membranes (PEMs). *Chemical Reviews Chem. Rev.* **2004**, *104*, 4587–4612.

17. Yang, C.; Costamagna, P.; Srinivasan, S.; Benziger, J.; Bocarsly, A. Approaches And Technical Challenges to High Temperature Operation of Proton Exchange Membrane Fuel Cells. *Journal of Power Sources*. **2001**, *103*, 1–9.

18. Tuckerman, M.; Laasonen, K.; Sprik, M.; Parrinello, M., The Journal of Chemical Physics. **1995**, 103 (1), 150-161.

19. M. E. Tuckerman, D. Marx and M. Parrinello, The nature and transport mechanism of hydrated hydroxide ions in aqueous solution, Nature **417** (2002) 925-929.

20. M. Schulze, E. Gülzow, *J. Power Sources* **2004**, 252.

21. Kinoshita, K. *Electrochemical Oxygen Technology*; Wiley: New York, 1992.

22. Kreuer, K. *Journal of Membrane Science*. **2001**, *185*, 29–39.

23. The Royal Society of Chemistry **Fuels Go Mobile**. http://www.rsc.org/chemistryworld/Issues/2003/January/mobile.asp (accessed March, 2016)

24. Merle, G.; Wessling, M.; Nijmeijer, K. *Journal of Membrane Science*. **2011**, *377*, 1–35.

25. Ran, J.; Wu, L.; Wei, B.; Chen, Y.; Xu, T. *Sci. Rep. Scientific Reports*. **2014**, *4*, 6486.

26. Varcoe, J. R.; Slade, R. C. T., Fuel Cells **2005**, 5 (2), 187-200

27. Cope, A. C.; Mehta, A. S. *J. Am. Chem. Soc. Journal of the American Chemical Society*. **1963**, *85*, 1949–1952.

28. J. B. Edson, C. S. Macomber, B. S. Pivovar and J. M. Boncella, *J. Membr. Sci*., **2012**, 399–400, 49–59.

29. Wang, G.; Weng, Y.; Chu, D.; Chen, R.; Xie, D. *Journal of Membrane Science*. **2009**, *332*, 63–68.

30. Zhang, Q.; Zhang, Q.; Wang, J.; Zhang, S.; Li, S. *Polymer*. **2010**, *51*, 5407–5416.

31. Pandey, A. K.; Goswami, A.; Sen, D.; Mazumder, S.; Childs, R. F. *Journal of Membrane Science*. **2003**, *217*, 117–130.

32. Guo, M.; Fang, J.; Xu, H.; Li, W.; Lu, X.; Lan, C.; Li, K. *Journal of Membrane Science*. **2010**, *362*, 97–104.

33. Kim, D. S.; Labouriau, A.; Guiver, M. D.; Kim, Y. S. *Chemistry of Materials Chem. Mater.* **2011**, *23*, 3795–3797.

34. Gu, S.; Cai, R.; Luo, T.; Jensen, K.; Contreras, C.; Yan, Y. *ChemSusChem*. **2010**, *3*, 555–558.

35. Noonan, K. J. T.; Hugar, K. M.; Kostalik, H. A.; Lobkovsky, E. B.; Abruña, H. D.; Coates, G. W. *J. Am. Chem. Soc*. **2012**, *134*, 18161–18164.

36. Zha, Y.; Disabb-Miller, M. L.; Johnson, Z. D.; Hickner, M. A.; Tew, G. N. *J. Am. Chem. Soc*. **2012**, *134*, 4493–4496.

37. Kreuer, K.-D. *Fuel Cells: Selected Entries from the Encyclopedia of Sustainability Science and Technology*; Springer, **2013**.

38. Li, Y.; Zhao, T.; Yang, W. *International Journal of Hydrogen Energy*. **2010**, *35*, 5656–5665.

39. *Ullmann's Polymers And Plastics Products and Processes*; Wiley-VCH: Weinheim, Germany, 2016.

40. Cotter, R. J. *Engineering Plastics: a Handbook of Polyarylethers*; Gordon and Breach: Basel, Switzerland, **1995**.

41. Mark, H. F. *Encyclopedia of Polymer Science and Technology*; John Wiley and Sonsm Inc.: Hoboken, New Jersey, **2003**; Vol. 4.

42. Ioan, S. *Functionalized Polysulfones: Synthesis, Characterization, Applications*; CRC Press.: Boca Raton, Florida, **2015**.

43. Kaiti, S.; Himmelber, P.; Williams, J.; Abdellatif, M.; Fossum, E. *Macromolecules* **2007**, 39, 7909.

44. Beek, D.V.; Fossum, E. *Macromolecules* **2009**, *42*, 4016-4022.

45. Tienda, K.; Yu, Z.; Constandinidis, F.; Fortney, A.; Feld, W.; Fossum, E. *J. Polym. Sci. Part A: Polym. Chem.* **2011**, 49, 2908-2915.

46. Selhorst, R.; Fossum, E. *Polymer*, **2013**, *54*, 530 - 535.

47. Dyson, R. W. *Speciality Polymers*; Blackie: Glasgow, **1987**.

48. Miyake, J.; Fukasawa, K.; Watanabe, M.; Miyatake, K. *J. Polym. Sci. Part A: Polym. Chem. Journal of Polymer Science Part A: Polymer Chemistry*. **2013**, *52*, 383–389.

49. Varcoe, J. R.; Atanassov, P.; Dekel, D. R.; Herring, A. M.; Hickner, M. A.; Kohl, P. A.; Kucernak, A. R.; Mustain, W. E.; Nijmeijer, K.; Scott, K.; Xu, T.; Zhuang, L. *Energy Environ. Sci.* **2014**, *7*, 3135–3191.

50. Zepf, V. *Rare earth elements: a new approach to the nexus of supply, demand and use - as exemplified by the use of neodymium in permanent magnets*; Springer: Berlin, **2013**.

51. Hu, F.; Lei, X. *ChemCatChem.* **2015**, *7* (10), 1539–1542.